Inclusive search for supersymmetry in pp collisions at $\sqrt{s} = 13$ TeV using razor variables and boosted object identification in zero and one lepton final states

The CMS collaboration

E-mail: cms-publication-committee-chair@cern.ch

ABSTRACT: An inclusive search for supersymmetry (SUSY) using the razor variables is performed using a data sample of proton-proton collisions corresponding to an integrated luminosity of $35.9\,\mathrm{fb}^{-1}$, collected with the CMS experiment in 2016 at a center-of-mass energy of $\sqrt{s} = 13$ TeV. The search looks for an excess of events with large transverse energy, large jet multiplicity, and large missing transverse momentum. The razor kinematic variables are sensitive to large mass differences between the parent particle and the invisible particles of a decay chain and help to identify the presence of SUSY particles. The search covers final states with zero or one charged lepton and features event categories divided according to the presence of a high transverse momentum hadronically decaying W boson or top quark, the number of jets, the number of b-tagged jets, and the values of the razor kinematic variables, in order to separate signal from background for a broad range of SUSY signatures. The addition of the boosted W boson and top quark categories within the analysis further increases the sensitivity of the search, particularly to signal models with large mass splitting between the produced gluino or squark and the lightest SUSY particle. The analysis is interpreted using simplified models of R-parity conserving SUSY, focusing on gluino pair production and top squark pair production. Limits on the gluino mass extend to 2.0 TeV, while limits on top squark mass reach 1.14 TeV.

KEYWORDS: Hadron-Hadron scattering (experiments), Supersymmetry

ARXIV EPRINT: 1812.06302

Contents

1   Introduction

We present an inclusive search for supersymmetry (SUSY) using the razor variables [1–3] on data collected by the CMS experiment in 2016. Supersymmetry extends space-time symmetry such that every fermion (boson) in the standard model (SM) has a bosonic (fermionic) partner [4–12]. Supersymmetric extensions of the SM yield solutions to the gauge hierarchy problem without the need for large fine tuning of fundamental parameters [13–18], exhibit gauge coupling unification [19–24], and can provide weakly interacting particle candidates for dark matter [25, 26].

The search described in this paper is an extension of previous work presented in refs. [2, 3]. The search is inclusive in scope, covering final states with zero or one charged

lepton. To enhance sensitivity to specific types of SUSY signatures, the events are categorized according to the presence of jets consistent with high transverse momentum (p_{T}) hadronically decaying W bosons or top quarks, the number of identified charged leptons, the number of jets, and the number of b-tagged jets. The search is performed in bins of the razor variables M_{R} and R^2 [1–3]. The result presented in this paper is the first search for SUSY from the CMS experiment that incorporates both Lorentz-boosted and "non-boosted" (resolved) event categories. This search strategy provides broad sensitivity to gluino and squark pair production in R-parity [27] conserving scenarios for a large variety of decay modes and branching fractions. The prediction of the SM background in the search regions (SRs) is obtained from Monte Carlo (MC) simulation calibrated with data control regions (CRs) that isolate the major background components. Additional validation of the assumptions made by the background estimation method yields estimates of the systematic uncertainties.

Other searches for SUSY by the CMS [28–36] and ATLAS [37–43] Collaborations have been performed using similar data sets and yield complementary sensitivity. Compared to those searches, the razor kinematic variables explore alternative signal-sensitive phase space and add robustness to the understanding of the background composition and the potential systematic uncertainties in the background models. To give a characteristic example, for squark pair production with a squark mass of 1000 GeV and a neutralino mass of 100 GeV, we find that the overlap of signal events falling in the most sensitive tail regions of the razor kinematic variables and of other kinematic variables used in alternative searches described in ref. [32] is 50–70%.

We present interpretations of the results in terms of production cross section limits for several simplified models [44–47] for which this search has enhanced sensitivity. The simplified models considered include gluino pair production, with each gluino decaying to a pair of top quarks and the lightest SUSY particle (LSP), referred to as "T1tttt"; gluino pair-production, with each gluino decaying to a top quark and a low-mass top squark that subsequently decays to a charm quark and the LSP, referred to as "T5ttcc"; and top squark pair production, with each top squark decaying to a top quark and the LSP, referred to as "T2tt". The corresponding diagrams for these simplified models are shown in figure 1. Although we only interpret the search results in a limited set of simplified models, the search can be sensitive to other simplified models that are not explicitly considered in this paper.

This paper is organized as follows. Details of the detector, trigger, and object reconstruction and identification are described in section 2. The MC simulation samples used to model background and signal processes are described in section 3. The analysis strategy and event categorization are discussed in section 4, and the background modeling is discussed in section 5. Systematic uncertainties are discussed in section 6, and finally the results and interpretations are presented in section 7. We summarize the paper in section 8.

2 The CMS detector and object reconstruction

The CMS detector consists of a superconducting solenoid of 6 m internal diameter, providing a magnetic field of 3.8 T. Within the solenoid volume there are a silicon pixel and
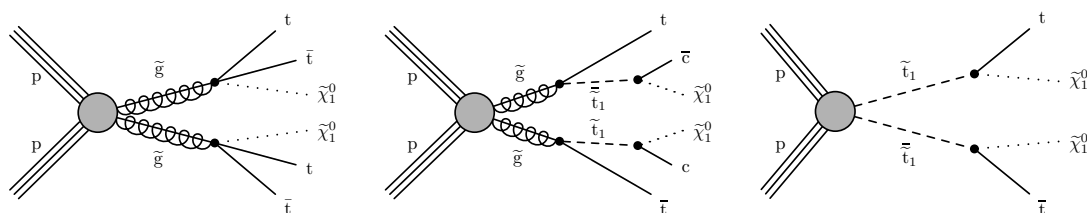
Figure 1. Diagrams for the simplified models considered in this analysis: (left) pair-produced gluinos, each decaying to two top quarks and the LSP, denoted T1tttt; (middle) pair-produced gluinos, each decaying to a top quark and a low mass top squark that subsequently decays to a charm quark and the LSP, denoted T5ttcc; (right) pair-produced top squarks, each decaying to a top quark and the LSP, denoted T2tt. In the diagrams, the gluino is denoted by $\widetilde{g}$, the top squark is denoted by $\widetilde{t}$, and the lightest neutralino is denoted by $\widetilde{\chi}_1^0$ and is the LSP.

a silicon strip tracker, a lead tungstate crystal electromagnetic calorimeter (ECAL), and a brass and scintillator hadron calorimeter (HCAL), each composed of a barrel and two endcap sections. Extensive forward calorimetry complements the coverage provided by the barrel and endcap detectors. Muons are measured in gas-ionization detectors embedded in the magnet steel flux-return yoke outside the solenoid. Events are selected by a two-level trigger system. The first level is based on a hardware filter, and the second level, the high level trigger, is implemented in software. A more detailed description of the CMS detector, together with a definition of the coordinate system used and the relevant kinematic variables, can be found in ref. [48].

Physics objects are defined using the particle-flow (PF) algorithm [49], which aims to reconstruct and identify each individual particle in an event using an optimized combination of information from the various elements of the CMS detector. Jets are clustered from PF candidates using the anti-k_T algorithm [50, 51] with a distance parameter of 0.4. Jet energy corrections are derived from simulation and confirmed by in-situ measurements of the energy balance in dijet, multijet, photon+jet, and leptonically decaying Z+jet events [52]. Further details of the performance of the jet reconstruction can be found in ref. [53]. Jets used in any selection of this analysis are required to have $p_\mathrm{T} > 30\,\mathrm{GeV}$ and pseudorapidity $|\eta| < 2.4$. To identify jets originating from b quarks, we use the "medium" working point of the combined secondary vertex (CSVv2) b jet tagger, which uses an inclusive vertex finder to select b jets [54]. The efficiency to identify a bottom jet is in the range of 50–65% for jets with p_T between 20 and 400 GeV, while the misidentification rate for light-flavor quark and gluon jets (charm jets) is about 1 (10)%. We also use the "loose" working point of the CSVv2 b jet tagger to identify b jets to be vetoed in the definition of various CRs. The loose b jet tagging working point has an efficiency of 80% and a misidentification rate for light-flavor and gluon jets of 10%.

Large-radius jets used for identifying Lorentz-boosted W bosons and top quarks are clustered using the anti-k_T algorithm with a distance parameter of 0.8. The subset of these jets having $|\eta| < 2.4$ and $p_\mathrm{T} > 200\,(400)\,\mathrm{GeV}$ are used to identify W bosons (top quarks). Identification is done using jet mass, the N-subjettiness variables [55], and subjet b tagging

for top quarks. Jet mass is computed using the soft-drop algorithm [56], and is required to be between 65–105 and 105–210 GeV for W bosons and top quarks, respectively. The N-subjettiness variables:

$$\tau_N = \frac{1}{d_0} \sum_k p_{\mathrm{T},k} \min\left(\Delta R_{1,k}, \Delta R_{2,k}, \cdots, \Delta R_{N,k}\right), \tag{2.1}$$

where N denotes candidate axes for subjets, k runs over all constituent particles, and $d_0 = R_0 \sum_k p_{\mathrm{T},k}$. R_0 is the clustering parameter of the original jet, and $\Delta R_{n,k}$ is the distance from constituent particle k to subjet n. The N-subjettiness variable is used to evaluate the consistency of a jet with having N subjets. To enhance discrimination, the ratios $\tau_{21} = \tau_2/\tau_1$ and $\tau_{32} = \tau_3/\tau_2$ are used for the W boson and top quark tagging, respectively, with the criteria of $\tau_{21} < 0.40$ and $\tau_{32} < 0.65$. For tagging top quarks ("t tagging"), an additional requirement is imposed on the subjet b tagging discriminant based on the multivariate CSVv2 algorithm [54]. The efficiencies for W boson and top quark tagging are on average 66 and 15%, respectively, with mistagging rates of 4.0 and 0.1% [53].

The missing transverse momentum vector $\vec{p}_{\mathrm{T}}^{\mathrm{miss}}$ is defined as the projection of the negative vector sum of the momenta of all reconstructed PF candidates on the plane perpendicular to the beams. Its magnitude is referred to as $p_{\mathrm{T}}^{\mathrm{miss}}$. Events containing signatures consistent with beam-induced background or anomalous noise in the calorimeters sometimes results in events with anomalously large values of $p_{\mathrm{T}}^{\mathrm{miss}}$ and are rejected using dedicated filters [57, 58]. The performance of the $p_{\mathrm{T}}^{\mathrm{miss}}$ at CMS may be found in ref. [59].

Electrons are reconstructed by associating an energy cluster in the ECAL with a reconstructed track [60], and are identified on the basis of the electromagnetic shower shape, the ratio of energies deposited in the ECAL and HCAL, the geometric matching of the track and the calorimeter cluster, the track quality and impact parameter, and isolation. To improve the efficiency for models that produce a large number of jets, a so-called "mini-isolation" technique is used, where the isolation cone shrinks as the momentum of the object increases. Further details are discussed in ref. [2]. Muons are reconstructed by combining tracks found in the muon system with corresponding tracks in the silicon tracking detectors [61], and are identified based on the quality of the track fit, the number of detector hits used in the tracking algorithm, the compatibility between track segments, and isolation. Two types of selections are defined for electrons and muons: a "tight" selection with an average efficiency of about 70–75%, and a "loose" selection with an efficiency of about 90–95%. The loose selections are required to have $p_{\mathrm{T}} > 5\,\mathrm{GeV}$, while the tight selections are required to have $p_{\mathrm{T}} > 30$ and $25\,\mathrm{GeV}$ for electrons and muons, respectively. Similarly electrons (muons) are required to have $|\eta| < 2.5$ (2.4), and electrons with $|\eta|$ (of 1.442–1.556) in the transition region between the barrel and endcap ECAL are not considered because of limited electron reconstruction capabilities in that region.

Hadronically decaying τ leptons (τ_{h}) are reconstructed using the hadron-plus-strips algorithm [62], which identifies τ lepton decay modes with one charged hadron and up to two neutral pions or three charged hadrons, and are required to be isolated. The "loose" selection used successfully reconstructs τ_{h} decays with an efficiency of about 50%. The reconstructed τ_{h} leptons have $p_{\mathrm{T}} > 20\,\mathrm{GeV}$ and $|\eta| < 2.4$.

Finally, photon candidates are reconstructed from energy clusters in the ECAL [63] and identified based on the transverse shower width, the hadronic to electromagnetic energy ratio in the HCAL and ECAL, and isolation. Photon candidates that share the same energy cluster as an identified electron are vetoed. Photons are used in the estimation of $Z \to \nu\nu$+jets backgrounds, and are required to have $|\eta| < 2.5$ and $p_\mathrm{T} > 185$ or $80\,\mathrm{GeV}$ for the non-boosted or boosted categories, respectively.

3   Simulation

Monte Carlo simulated samples are used to predict the SM backgrounds in the SRs and to calculate the selection efficiencies for SUSY signal models. Events corresponding to the Z+jets, γ+jets, and quantum chromodynamics (QCD) multijet background processes, as well as the SUSY signal processes, are generated at leading order with MadGraph5_amc@nlo 2.2.2 [64, 65] interfaced with pythia V8.205 [66] for fragmentation and parton showering, and matched to the matrix element kinematic configuration using the MLM algorithm [67, 68]. The CUETP8M1 pythia 8 tune [69] was used. Other background processes are generated at next-to-leading order (NLO) with Mad-Graph5_amc@nlo 2.2.2 [65] (W+jets, s-channel single top quark, $t\bar{t}W$, $t\bar{t}Z$ processes) or with powheg v2.0 [70–72] ($t\bar{t}$+jets, t-channel single top quark, and tW production), both interfaced with pythia V8.205. Simulated samples generated at LO (NLO) used the NNPDF3.0LO (NNPDF3.0NLO) [73] parton distribution functions. The SM background events are simulated using a Geant4-based model [74] of the CMS detector, while SUSY signal events are simulated using the CMS fast simulation package [75]. All simulated events include the effects of pileup, multiple pp collisions within the same or neighboring bunch crossings.

The SUSY particle production cross sections are calculated to NLO plus next-to-leading-log (NLL) precision [76–81] with all other sparticles assumed to be heavy and decoupled. The NLO+NLL cross sections and their associated uncertainties from ref. [81] are taken as a reference to derive the exclusion limit on the SUSY particle masses.

To improve on the MadGraph5_amc@nlo modeling of the multiplicity of additional jets from initial-state radiation (ISR), strongly produced SUSY signal samples are reweighted as a function of the number of ISR jets ($N_\mathrm{jets}^\mathrm{ISR}$). This correction is derived from a $t\bar{t}$ enriched control sample such that the jet multiplicity from the MadGraph5_amc@nlo-generated $t\bar{t}$ sample agrees with data. The reweighting factors vary between 0.92 and 0.51 for $N_\mathrm{jets}^\mathrm{ISR}$ between one and six. We take one half of the deviation from unity as the systematic uncertainty in these reweighting factors.

4   Analysis strategy and event categorization

We perform the search in several event categories defined according to the presence of jets tagged as originating from a boosted hadronic W boson or top quark, the number of identified charged leptons, jets, and b-tagged jets. A summary of the categories used is shown in table 1 below.

Category	Lepton requirement	Jet requirement	b tag bins
Lepton multijet	1 "Tight" electron or muon	4–6 jets	0, 1, 2, ≥ 3 b tags
Lepton seven-jet	1 "Tight" electron or muon	≥ 7 jets	0, 1, 2, ≥ 3 b tags
Boosted W 4–5 jet	Lepton veto	≥ 1 W-tagged jet 4–5 jets	≥ 1 b tags
Boosted W 6 jet	Lepton veto	≥ 1 W-tagged jet ≥ 6 jets	≥ 1 b tags
Boosted top	Lepton veto	0 W-tagged jets ≥ 1 t-tagged jet ≥ 6 jets	≥ 0 b tags
Dijet	Lepton veto	0 W-tagged jets 0 t-tagged jets 2–3 jets	0, 1, ≥ 2 b tags
Multijet	Lepton veto	0 W-tagged jets 0 t-tagged jets 4–6 jets	0, 1, 2, ≥ 3 b tags
Seven-jet	Lepton veto	0 W-tagged jets 0 t-tagged jets ≥ 7 jets	0, 1, 2, ≥ 3 b tags

Table 1. Summary of the search categories, their charged lepton and jet count requirements, and the b tag bins that define the subcategories. Events passing the "Lepton veto" requirement must have no electron or muon passing the loose selection, and no τ_h candidate.

Events in the one-lepton category are required to have one and only one charged lepton (electron or muon), with p_T above $30\,(25)\,\mathrm{GeV}$ for electrons (muons) selected using the tight criteria, while events in the zero-lepton category are required to have no electrons or muons passing the loose selection criteria and no τ_h candidates. One-lepton events are placed in the "Lepton Multijet" category if they have between 4 and 6 jets, and placed in the "Lepton Seven-jet" category if they have 7 or more jets. One-lepton events with fewer than 4 jets are not considered in the analysis.

Zero-lepton events with jets tagged as originating from a boosted hadronic W boson or top quark decay are placed in a dedicated "boosted" event category. Events in this "boosted" category are analyzed separately with a set of CRs and validation tests specific for the analysis with boosted objects. They are further classified into those having at least one tagged W boson and one tagged b jet ("W" category), and those having at least one tagged top quark ("Top" category). Events in the W category are further divided into subcategories with 4–5 jets, and 6 jets or more. Zero-lepton events not tagged as having boosted W bosons or top quarks are placed into the "Dijet" category if they have two or three jets, the "Multijet" category if they have between 4 and 6 jets, and into the "Seven-jet" category if they have 7 or more jets.

The Dijet category is further divided into subcategories with zero, one, and two or more b-tagged jets, and all other non-boosted categories are divided into subcategories with zero, one, two, and three or more b-tagged jets.

For each event in the above categories, we group the selected charged leptons and jets in the event into two distinct hemispheres called megajets, whose four-momenta are defined as the vector sum of the four-momenta of the physics objects in each hemisphere. The clustering algorithm selects the grouping that minimizes the sum of the squared invariant masses of the two megajets [82]. We define the razor variables M_R and M_T^R as:

$$M_R \equiv \sqrt{(|\vec{p}^{\,j1}| + |\vec{p}^{\,j2}|)^2 - (p_z^{j1} + p_z^{j2})^2}, \tag{4.1}$$

$$M_T^R \equiv \sqrt{\frac{p_T^{miss}(p_T^{j1} + p_T^{j2}) - \vec{p}_T^{\,miss} \cdot (\vec{p}_T^{\,j1} + \vec{p}_T^{\,j2})}{2}}, \tag{4.2}$$

where $\vec{p}^{\,ji}$, $\vec{p}_T^{\,ji}$, and p_z^{ji} are the momentum of the i-th megajet, its transverse component with respect to the beam axis, and its longitudinal component, respectively. The dimensionless variable R is defined as:

$$R \equiv \frac{M_T^R}{M_R}. \tag{4.3}$$

For pair-produced SUSY signals, the variable M_R quantifies the mass splitting between the pair-produced particle and the LSP, and exhibits a peaking structure, while for background it is distributed as an exponentially decaying spectrum. The variable R quantifies the degree of imbalance between the visible and invisible decay products and helps to suppress backgrounds which do not produce any weakly interacting particles. The combination of the two variables provide powerful discrimination between the SUSY signal and SM backgrounds.

Single-electron or single-muon triggers are used to collect events in the one-lepton categories, with a total trigger efficiency of about 80% for reconstructed p_T around 30 GeV, growing to 95% for reconstructed p_T above 50 GeV. Events in the boosted category are collected using triggers that select events based on the p_T of the leading jet and the scalar p_T sum of all jets, H_T. The trigger efficiency is about 50% at the low range of the M_R and R^2 kinematic variables and grows to 100% for $M_R > 1.2$ TeV and $R^2 > 0.16$. For the zero-lepton non-boosted event categories, dedicated triggers requiring at least two jets with $p_T > 80$ GeV and loose thresholds on the razor variables M_R and R^2 are used to collect the events. The trigger efficiency ranges from 95–100% and increases with M_R and R^2.

Preselection requirements on the M_R and R^2 variables are made depending on the event category. For events in the one-lepton categories, further requirements are made on the transverse mass m_T defined as follows:

$$m_T = \sqrt{2p_T^{miss}p_T^\ell[1 - \cos(\Delta\phi)]}, \tag{4.4}$$

where p_T^ℓ is the charged-lepton transverse momentum, and $\Delta\phi$ is the azimuthal angle (in radians) between the charged-lepton momentum and the p_T^{miss}. For events in the zero-lepton categories, further requirements are made on the azimuthal angle $\Delta\phi_R$ between the axes of the two razor megajets. These requirements are summarized in table 2.

Finally, in each event category, the search is performed in bins of the kinematic variables M_R and R^2 in order to take advantage of the varying signal-to-background ratio in

Category	Preselection	Additional requirements	Trigger requirement
Lepton multijet	$M_R > 550\,\text{GeV}$ & $R^2 > 0.20$	$m_T > 120\,\text{GeV}$	Single lepton
Lepton seven-jet	$M_R > 550\,\text{GeV}$ & $R^2 > 0.20$	$m_T > 120\,\text{GeV}$	Single lepton
Boosted W 4–5 jet	$M_R > 800\,\text{GeV}$ & $R^2 > 0.08$	$\Delta\phi_R < 2.8$	H_T, jet p_T
Boosted W 6 jet	$M_R > 800\,\text{GeV}$ & $R^2 > 0.08$	$\Delta\phi_R < 2.8$	H_T, jet p_T
Boosted top	$M_R > 800\,\text{GeV}$ & $R^2 > 0.08$	$\Delta\phi_R < 2.8$	H_T, jet p_T
Dijet	$M_R > 650\,\text{GeV}$ & $R^2 > 0.30$	$\Delta\phi_R < 2.8$	Hadronic razor
Multijet	$M_R > 650\,\text{GeV}$ & $R^2 > 0.30$	$\Delta\phi_R < 2.8$	Hadronic razor
Seven-jet	$M_R > 650\,\text{GeV}$ & $R^2 > 0.30$	$\Delta\phi_R < 2.8$	Hadronic razor

Table 2. The baseline requirements on the razor variables M_R and R^2, additional requirements on m_T and $\Delta\phi_R$, and the trigger requirements are shown for each event category.

the different bins. For one-lepton categories, the SRs are composed of five bins in M_R, starting from 550 GeV, and five bins in R^2 starting from 0.20. For the zero-lepton boosted categories, the SRs are composed of five bins in M_R, starting from 800 GeV, and five bins in R^2, starting from 0.08. Finally, for the zero-lepton non-boosted categories, the SRs are composed of five bins in M_R, starting from 650 GeV, and four bins in R^2 starting from 0.30. To match with the expected resolution, the bin widths in M_R increases from 100 to 300 GeV as the value of M_R grows from 400 to 1200 GeV. In each category, to limit the impact of statistical uncertainties due to the limited size of the MC simulation samples, bins are merged such that the expected background in each bin is larger than about 0.1 events. As a result, the SRs have a decreasing number of bins as the number of jets, b-tagged jets, and M_R increases.

5 Background modeling

The main background processes in the SRs considered are $W(\ell\nu)$+jets (with $\ell = e, \mu, \tau$), $Z(\nu\overline{\nu})$+jets, $t\overline{t}$, and QCD multijet production. For event categories with zero b-tagged jets, the background is primarily composed of the $W(\ell\nu)$+jets and $Z(\nu\overline{\nu})$+jets processes, while for categories with two or more b-tagged jets it is dominated by the $t\overline{t}$ process. There are also small contributions at the level of a few percent from single top quark production, production of two or three electroweak bosons, and production of $t\overline{t}$ in association with a W or Z boson.

The background prediction strategy relies on the use of CRs to isolate each background process, address deficiencies of the MC simulation using control samples in data, and estimate systematic uncertainties in the expected event yields. The CRs are defined such that they have no overlap with any SRs. For the dominant backgrounds discussed above, the primary sources of mismodeling come from inaccuracy in the MC prediction of the hadronic recoil spectrum and the jet multiplicity. Corrections to the MC simulation are applied first in bins of M_R and R^2, and then subsequently in the number of jets (N_{jets}) to address these modeling inaccuracies. The CR bins generally follow the bins of the SRs described in section 4, but bins with limited statistical power are merged in order to avoid large statistical fluctuations in the background predictions.

For the boosted categories, the CR selection and categorization are slightly adapted and the details are discussed further in section 5.4. An additional validation of the background prediction method is also performed for the boosted categories.

In what follows, all background MC samples are corrected for known mismodeling of the jet energy response, the trigger efficiency, and the selection efficiency of electrons, muons, and b-tagged jets. These corrections are mostly in the range of 0–5%, but can be as large as 10% in bins with large M_{R} and R^2, where the corrections have larger statistical uncertainties.

5.1 The $t\bar{t}$ and $\mathrm{W}(\ell\nu)$+jets backgrounds

We predict the $t\bar{t}$ and $\mathrm{W}(\ell\nu)$ backgrounds from the MC simulation corrected for inaccuracies in the modeling of the hadronic recoil. The corrections are derived in a CR consisting of events having at least one tight electron or muon. In order to separate the CR from the SRs and to reduce the QCD multijet background, the $p_{\mathrm{T}}^{\mathrm{miss}}$ is required to be larger than 30 GeV, and m_{T} is required to be between 30 and 100 GeV.

The tight lepton control sample is separated into $\mathrm{W}(\ell\nu)$+jets-enriched and $t\bar{t}$-enriched samples by requiring events to have zero (for $\mathrm{W}(\ell\nu)$+jets), or one or more (for $t\bar{t}$) b-tagged jets, respectively. The purity of the $\mathrm{W}(\ell\nu)$+jets and $t\bar{t}$ dominated CRs are both about 80%. In each sample, corrections to the MC prediction are derived in two-dimensional bins in M_{R} and R^2. The contribution from all other background processes estimated from simulation in each bin in a given CR ($N_{\mathrm{CR\ bin\ }i}^{\mathrm{MC,bkg}}$) is subtracted from the data yield in the corresponding bin in the CR ($N_{\mathrm{CR\ bin\ }i}^{\mathrm{data}}$), and compared to the MC prediction ($N_{\mathrm{CR\ bin\ }i}^{\mathrm{MC,}t\bar{t}}$) to derive the correction factor:

$$C_{\mathrm{bin\ }i}^{t\bar{t}} = \frac{N_{\mathrm{CR\ bin\ }i}^{\mathrm{data}} - N_{\mathrm{CR\ bin\ }i}^{\mathrm{MC,bkg}}}{N_{\mathrm{CR\ bin\ }i}^{\mathrm{MC,}t\bar{t}}}. \tag{5.1}$$

Finally, the prediction for the $t\bar{t}$ background in the SR ($N_{\mathrm{SR\ bin\ }i}^{t\bar{t}}$) is:

$$N_{\mathrm{SR\ bin\ }i}^{t\bar{t}} = N_{\mathrm{SR\ bin\ }i}^{\mathrm{MC,}t\bar{t}} C_{\mathrm{bin\ }i}^{t\bar{t}}, \tag{5.2}$$

where $N_{\mathrm{SR\ bin\ }i}^{\mathrm{MC,}t\bar{t}}$ is the prediction for the SR from the MC simulation.

Because the $t\bar{t}$-enriched sample is the purer of the two, the corrections are first derived in this sample. These corrections are applied to the $t\bar{t}$ simulation in the $\mathrm{W}(\ell\nu)$+jets-enriched sample, and then analogous corrections and predictions for the $\mathrm{W}(\ell\nu)$+jets background process are derived.

The corrections based on M_{R} and R^2 are measured and applied by averaging over all jet multiplicity bins. As our SRs are divided according to the jet multiplicity, additional corrections are needed in order to ensure correct background modeling for different numbers of jets. We derive these corrections separately for the $t\bar{t}$ and $\mathrm{W}(\ell\nu)$+jets samples, obtaining correction factors for events with two or three jets, four to six jets, and seven or more jets. The $t\bar{t}$ correction is derived prior to the $\mathrm{W}(\ell\nu)$+jets correction to take advantage of the slightly higher purity of the $t\bar{t}$ CR.

We also check for MC mismodeling that depends on the number of b jets in the event. To do this we apply the above-mentioned corrections in bins of M_R, R^2, and the number of jets and derive an additional correction needed to make the predicted M_R spectrum match that in data for each b tag multiplicity. This correction is performed separately for events with two or three, four to six, and seven or more jets.

A final validation of the MC modeling in this tight lepton CR is completed by comparing the R^2 spectrum in data with the MC prediction in each jet multiplicity and b tag multiplicity category. We do not observe any systematic mismodeling in the R^2 spectra, and we propagate the total uncertainty in the data-to-MC ratio in each bin of R^2 as a systematic uncertainty in the $t\bar{t}$ and W+jets backgrounds in the analysis SRs.

The $t\bar{t}$ background in the tight lepton CR is composed mostly of lepton+jets $t\bar{t}$ events, where one top quark decayed fully hadronically and the other top quark decayed leptonically. In the leptonic analysis SRs, the m_T requirement suppresses lepton+jets $t\bar{t}$ events, and the dominant remaining $t\bar{t}$ background consists of $t\bar{t}$ events where both top quarks decayed leptonically, and one of the two leptons is not identified. It is therefore important to validate that the corrections to the $t\bar{t}$ simulation derived in the tight lepton CR also describe dileptonic $t\bar{t}$ events well. We perform this check by selecting an event sample enriched in dileptonic $t\bar{t}$ events, applying the corrections on the $t\bar{t}$ simulation prediction derived in the tight lepton CR, and evaluating the consistency of the data with the corrected prediction. This check is performed separately for each jet multiplicity category used in the analysis SRs. The dilepton $t\bar{t}$-enriched sample consists of events with two tight electrons or muons with $p_T > 30\,\text{GeV}$ and invariant mass larger than $20\,\text{GeV}$, at least one b-tagged jet with $p_T > 40\,\text{GeV}$, and $p_T^{\text{miss}} > 40\,\text{GeV}$. Events with two same-flavor leptons with invariant mass between 76 and $106\,\text{GeV}$ are rejected to suppress Drell-Yan background. The p_T^{miss} and the m_T variables are computed treating one of the leptons in each event as visible and the other as invisible, and the requirement on the m_T is subsequently applied. A systematic uncertainty in the dilepton $t\bar{t}$ background is assessed by comparing data with the MC prediction in the M_R distribution for each jet multiplicity category. The M_R distributions in the $t\bar{t}$ dilepton CR for the two to three and four to six jet event categories are displayed in the upper row of figure 2.

The MC prediction for the hadronic SRs can be affected by potential mismodeling of the identification efficiency for electrons, muons, and τ_h candidates. The loose lepton and τ_h CRs are defined in order to assess the modeling of this efficiency in simulation. Events in the loose lepton (τ_h) CR are required to have at least one loose electron or muon (τ_h candidate) and pass one of the hadronic razor triggers. These events must also have m_T between 30 and $100\,\text{GeV}$, $M_R > 400\,\text{GeV}$, $R^2 > 0.25$, and at least two jets with $p_T > 80\,\text{GeV}$. The data and MC prediction are compared in bins of lepton p_T and η for each jet multiplicity category. A systematic uncertainty of about 25% is assigned to cover the difference between data and prediction in the lepton p_T spectrum. No further systematic mismodeling is observed in the lepton η distributions, and the size of the uncertainty in each η bin is propagated as an uncertainty in the analysis SR predictions. The lepton p_T distributions obtained in the loose lepton CR for the categories with two to three and four to six jets are displayed in the lower row of figure 2.
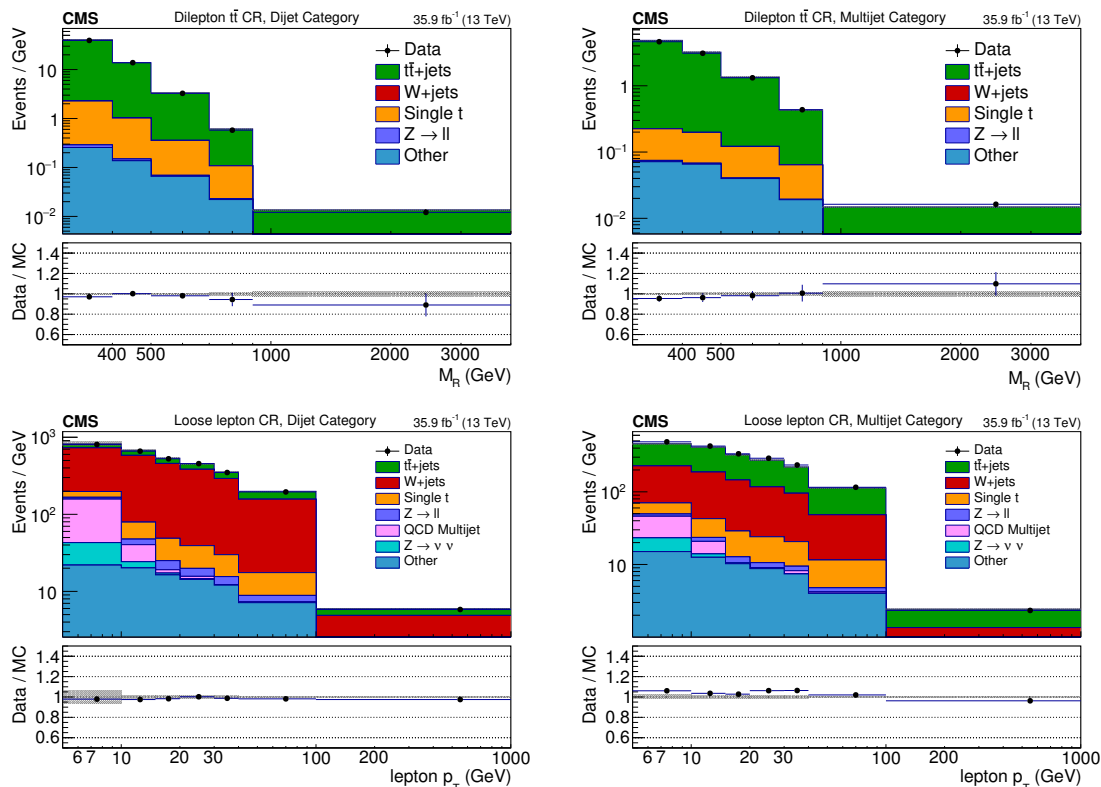
Figure 2. The M_R distribution in the $t\bar{t}$ dilepton CR (upper row) and lepton p_T distribution in the loose lepton CR (lower row) are displayed in the 2–3 (left) and 4–6 (right) jet categories along with the corresponding MC predictions. The corrections derived from the $t\bar{t}$ and W+jets CR have been applied. The ratio of data to the MC prediction is shown on the bottom panel, with the statistical uncertainty expressed through the data point error bars and the systematic uncertainty in the background prediction represented by the shaded region.

5.2 The $Z \to \nu\bar{\nu}$ background

The background prediction for the $Z(\nu\bar{\nu})$+jets process is made using the same methodology as for the $t\bar{t}$ and $W(\ell\nu)$ background processes. We take advantage of the kinematic similarities between the $Z \to \ell\ell$, $W(\ell\nu)$+jets, and γ+jets processes [83–85]. Corrections to the hadronic recoil and jet multiplicity spectra are obtained in a control sample enriched in γ+jets events, and the validity of these corrections is checked in a second control sample enriched in $W(\ell\nu)$+jets events. A third control sample, enriched in $Z \to \ell\ell$ events, is used to normalize the obtained correction factors and to provide an additional consistency check of the MC prediction.

The γ+jets control sample consists of events having at least one selected photon and passing a set of kinematic requirements. Photons are required to have $p_T > 185$ GeV and pass loose identification and isolation criteria. The photon is treated as invisible — its p_T is added vectorially to the $\vec{p}_T^{\,miss}$, and it is ignored in the calculation of M_R — in order to simulate the invisible Z boson decay products in a $Z \to \nu\bar{\nu}$+jets event. Selected events must pass a single-photon trigger, have two jets with $p_T > 80$ GeV, and have $M_R > 400$ GeV and $R^2 > 0.25$.

The contribution of misidentified photons to the yield in this control sample is estimated via a template fit to the distribution of the photon charged isolation, the p_T sum of all charged PF particles within a ΔR cone of size 0.4 centered on the photon momentum axis. The fit is performed in bins of M_R and R^2 and yields an estimate of the purity of the photon sample in each bin. Contributions from other background processes such as $t\bar{t}\gamma$ are estimated using simulation and account for about 1–2%. Additionally, events in which the photon is produced within a jet are considered to be background. Corrections to the hadronic recoil in simulation are derived in this CR by subtracting the estimated background yields from the number of observed counts, and comparing the resulting yield with the prediction from the γ+jets simulation, in each bin of M_R and R^2.

As in the tight lepton CR described in section 5.1, an additional correction is derived to account for possible mismodeling in simulation as a function of the jet multiplicity. This correction is derived for events with two or three jets, with four to six jets, and with seven or more jets. After these corrections are applied, the data in the CR are compared with the MC prediction in bins of the number of b-tagged jets. As in the tight lepton CR, the M_R spectra in simulation are corrected to match the data in each b tag category, and a systematic uncertainty in the $Z(\nu\bar{\nu})$+jets background is assigned based on the size of the uncertainty in each bin of R^2.

A check of the $Z(\nu\bar{\nu})$+jets prediction is performed with a sample enriched in $Z \to \ell\ell$ decays. Events in this sample are required to have two tight electrons or two tight muons having an invariant mass consistent with the Z mass. The two leptons are treated as invisible for the purpose of computing the razor variables. Events must have no b-tagged jets, two or more jets with $p_T > 80\,\text{GeV}$, $M_R > 400\,\text{GeV}$, and $R^2 > 0.25$. The correction factors obtained from the γ+jets CR are normalized so that the total MC prediction in the $Z \to \ell^+\ell^-$+jets CR matches the observed data yield. This corrects for the difference between the true γ+jets cross section and the leading order cross section used to normalize the simulated samples. The M_R distributions in this CR for the two to three and four to six jet categories are shown in figure 3. The observed residual disagreements between data and simulation in the M_R and R^2 distributions are propagated as systematic uncertainties in the $Z(\nu\bar{\nu})$+jets prediction.

The MC corrections derived in the γ+jets CR are checked against a second set of corrections derived in a CR enriched in $W(\ell\nu)$+jets events. This CR is identical to the $W(\ell\nu)$+jets sample described in section 5.1, except that the selected lepton is treated as invisible for the purpose of computing M_R and R^2. Correction factors are derived in the same way as in the $W(\ell\nu)$+jets CR. The full difference between these corrections and those obtained from the γ+jets CR is taken as a systematic uncertainty in the $Z(\nu\bar{\nu})$+jets prediction in the SR, and is typically between 10 and 20%, depending on the bin.

5.3 The QCD multijet background

Multijet events compose a nonnegligible fraction of the total event yield in the hadronic SRs. Such events are characterized by a significant undermeasurement of the energy of a jet, and consequently a large amount of p_T^{miss}, usually pointing towards the mismeasured jet. A large fraction of QCD multijet events are rejected by the requirement that the

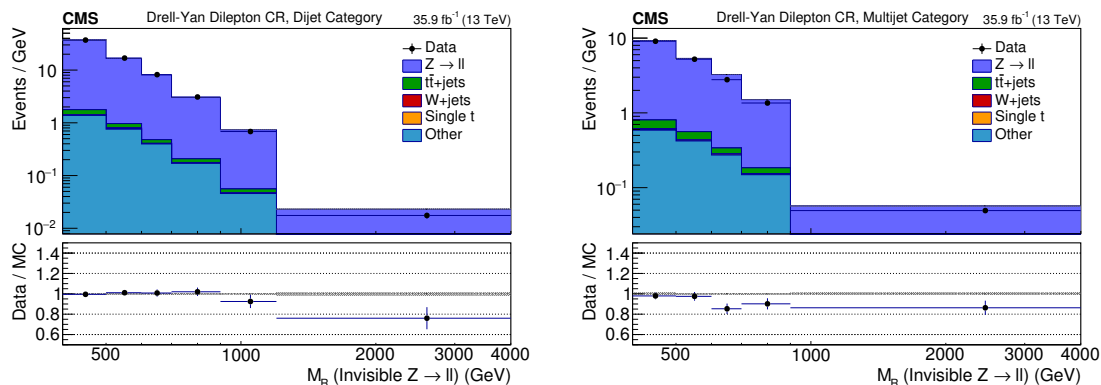**Figure 3**. The M_R distribution in the $Z \to \ell\ell$+jets CR is displayed in the 2–3 (left) and 4–6 (right) jet categories along with the corresponding MC predictions. The corrections derived from the γ+jets CR, as well as the overall normalization correction, have been applied in this figure.

azimuthal angle $\Delta\phi_R$ between the axes of the two razor megajets is less than 2.8. We treat the events with $\Delta\phi_R \geq 2.8$ as a CR of QCD multijet events, while the events with $\Delta\phi_R < 2.8$ define the SRs.

We estimate the number of QCD multijet events in this CR in bins of M_R and R^2 by subtracting the predicted contribution of other processes from the total event yield in each bin. This is done for each jet multiplicity category. We observe in simulation that the fraction of QCD multijet events at each b tag multiplicity is independent of M_R, R^2, and $\Delta\phi_R$. The event yields in the QCD CRs are therefore measured inclusively in the number of b tags and then scaled according to the fraction of QCD multijet events at each multiplicity of b-tagged jets.

We then predict the number of QCD multijet events in the SRs via the transfer factor ζ, defined as

$$\zeta = \frac{N(|\Delta\phi_R| < 2.8)}{N(|\Delta\phi_R| > 2.8)}. \tag{5.3}$$

It is calculated using control regions in data and validated with simulation. The QCD background prediction in each bin ($N_{SR\ bin\ i}^{QCD}$) is made as:

$$N_{SR\ bin\ i}^{QCD} = \zeta(N_{CR\ bin\ i}^{data} - N_{CR\ bin\ i}^{bkg}), \tag{5.4}$$

where $N_{CR\ bin\ i}^{data}$ is the number of events observed in the data CR and $N_{CR\ bin\ i}^{bkg}$ is the contribution from background processes other than the QCD multijet process and is predicted from the corrected MC.

We observe in simulation that ζ changes slowly with M_R and increases roughly linearly with R^2. In data we therefore compute ζ in bins of M_R and R^2 in a low-R^2 region defined by $0.20 < R^2 < 0.30$ and fit the computed values with a linear function in M_R and R^2. We then use the linear fit and its uncertainty to estimate the value of ζ in the analysis SRs. The fit is performed separately in each category of jet multiplicity, but inclusively in the number of b-tagged jets, as ζ is observed in simulation not to depend on the b tag multiplicity. For the category with seven or more jets, the fit function is allowed to depend on R^2 only, because of the low number of events in the fit region.

The statistical uncertainty in the CR event counts and the fitted uncertainty of the transfer factor extrapolation are propagated as systematic uncertainties of the QCD multijet background prediction. Another systematic uncertainty of 30% is propagated in order to cover the dependence of the transfer factor on the number of b-tagged jets in different CRs. Furthermore, we make an alternative extrapolation for the transfer factor where we allow a dependence on M_R and R^2 for the Seven-jet category, and a quadratic dependence on M_R for the Dijet and Multijet categories. The difference in the QCD multijet background prediction between the default and alternative transfer factor extrapolation is propagated as an additional systematic uncertainty, whose size ranges from 10% for M_R below 1 TeV to 70–90% for M_R above 1.6 TeV.

5.4 Background modeling in boosted event categories

The dominant SM background processes in the boosted categories are the same as in the non-boosted categories. An additional, but important source of background comes from processes where one of the jets in the event is mistagged as a boosted hadronic W boson or top quark.

Requiring boosted objects in the selection results in a smaller number of events in the SRs or CRs. As a general rule, in cases where no MC events exist in SR bins for a given background process, MC counts in these bins are extrapolated from a looser version of the signal selection obtained by relaxing the N-subjettiness criteria for W or t tagging. For cases where there are no counts or very low statistical precision in the CR bins, these depleted bins are temporarily merged to obtain coarser bins with increased event count. Background estimation is done in two steps, where first the yields are estimated using the coarser bins, and next, the yields in coarse bins are distributed to the finer bins proportional to the background MC counts in the finer bins.

5.4.1 The $t\bar{t}$+jets and W+jets background estimation for the boosted categories

The CRs for the $t\bar{t}$ and W+jets backgrounds are defined similar to the CRs used for the non-boosted categories. We require exactly one loose electron or muon. To suppress contamination from signal processes, m_T is required to be less than 100 GeV. To mimic the signal selection, the $\Delta\phi_R < 2.8$ requirement is applied. To estimate the top quark background for the boosted W 4–5 jet and boosted W 6 jet SR categories, we require events in the CR to have at least one boosted W boson and one b-tagged jet, while for the boosted top category, we require one boosted top quark. To estimate the W($\ell\nu$)+jets background for the boosted W 4–5 jet and boosted W 6 jet SR categories, we require events in the CR to have no loosely tagged b jets, while for the boosted top category we require no b-tagged subjets. To maintain consistency with SR kinematics, we require a jet which is tagged only using the W boson or top quark mass requirement, but without the N-subjettiness requirement. The background estimate for each SR i is then extrapolated from the corresponding CR via transfer factors calculated in MC: $\lambda_i = N_i^{\text{SR,MC}}/N_i^{\text{CR,MC}}$.

For certain bins, the MC prediction of the transfer factors can have large statistical fluctuations from the limited number of MC events. To smooth out these fluctuations we use
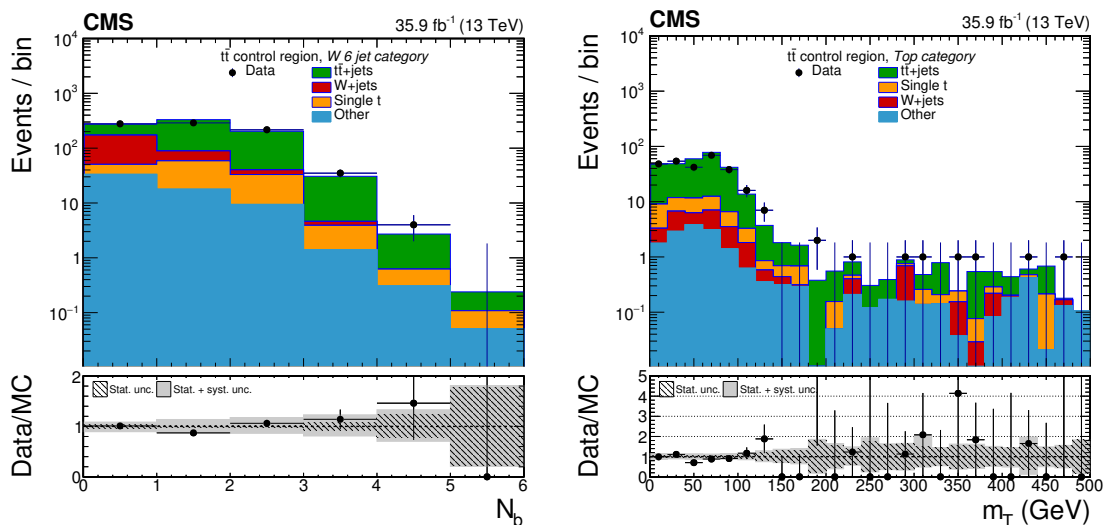
Figure 4. The distribution of b-tagged jet multiplicity before applying the b tagging selection requirement in the $t\bar{t}$ CR of the boosted W 6 jet category (left), and the distribution in m_T before applying the m_T selection requirement in the $t\bar{t}$ CR of the boosted top category (right) are shown. The ratio of data over MC prediction is shown in the lower panels, where the gray band is the total uncertainty and the dashed band is the statistical uncertainty in the MC prediction.

a combination of bin-merging and extrapolations from a region with looser requirements on the N-subjettiness variables. While the fluctuations in the nominal background prediction are smoothed out, the statistical uncertainties from the limited MC sample size are still propagated as a systematic uncertainty.

Figure 4 shows the b-tagged jet multiplicity distribution, identified with the medium b jet tagger, for events in the boosted W 6 jet category in the $t\bar{t}$ CR before applying the b tagging selection, and the m_T distribution in the boosted top category in the $t\bar{t}$ CR before applying the m_T selection. Figure 5 shows the distribution in M_R and R^2 bins for events in the boosted top category in the $t\bar{t}$ CR, and for events in the boosted W 4–5 jet and boosted W 6 jet categories in the W($\ell\nu$)+jets CR. The purity of $t\bar{t}$+jets and single top events in the $t\bar{t}$ CR is more than 80%, and the purity of the W($\ell\nu$)+jets process in the W($\ell\nu$)+jets CR is also larger than 80%.

5.4.2 The $Z \rightarrow \nu\bar{\nu}$+jets background estimation for the boosted categories

The background estimate for the $Z \rightarrow \nu\bar{\nu}$+jets process is again similar to the method used for the non-boosted categories. We make use of the similarity in the kinematics of the photon in γ+jets events and the Z boson in Z+jets events to select a control sample of γ+jets to mimic the behavior of $Z \rightarrow \nu\bar{\nu}$+jets events. The γ+jets CR is selected by requiring exactly one photon with $p_T > 80\,\text{GeV}$ from data collected by jet and H_T triggers. The momentum of the photon is added to $\vec{p}_T^{\,\text{miss}}$ to mimic the contribution of the neutrinos from $Z \rightarrow \nu\bar{\nu}$ decays. We require that the events contain no loose leptons or τ_h candidates, and $\Delta\phi_R$, computed after treating the photon as invisible, is required to be less than 2.8. One W-tagged or t-tagged jet is required for the boosted W and top categories,

Figure 5. M_R–R^2 distributions in the W+jets CRs of the boosted W 4–5 jet (upper left) and boosted W 6 jet (upper right) categories, and the $t\bar{t}$ CR (lower) of the boosted top category. The ratio of data over MC prediction is shown in the lower panels, where the gray band is the total uncertainty and the dashed band is the statistical uncertainty in the MC prediction.

respectively. Figure 6 shows the M_R–R^2 distribution for the boosted top category. The QCD multijet contribution to the γ+jets CR is accounted for by a template fit to the photon charged isolation variable in inclusive bins of M_R and R^2. Other background processes in the γ+jets CRs are small and predicted using MC. Finally, the SR prediction for the $Z \to \nu\bar{\nu}$+jets background is extrapolated from the γ+jets yields via the MC transfer factor $\lambda_{Z \to \nu\bar{\nu}} = N_{Z \to \nu\bar{\nu}}^{\mathrm{SR,MC}} / N_{\gamma+\mathrm{jets}}^{\mathrm{CR,MC}}$.

Figure 6. M_R–R^2 distributions for the γ+jets CR of the boosted W 4–5 jet (left) and boosted top (right) category. The ratio of data over MC prediction is shown in the lower panel, where the gray band is the total uncertainty and the dashed band is the statistical uncertainty in the MC prediction.

We perform a cross check on the previous estimate using a CR enhanced in $Z \to \ell\ell$ events. The $Z \to \ell\ell$ CR is defined by requiring exactly two tight electrons or muons with $p_T > 10\,\text{GeV}$ and dilepton mass satisfying $|m_{\ell\ell} - m_Z| < 10\,\text{GeV}$, where m_Z is the Z boson mass. All other requirements are the same as those for the γ+jets CR. The momentum of the dilepton system is added vectorially to $\vec{p}_T^{\,\text{miss}}$ to mimic an invisible decay of the Z boson. Similarly for the non-boosted categories, the comparison between data and MC yields in the $Z \to \ell\ell$ CR are used to correct the MC transfer factor λ to account for the impact of missing higher order corrections on the total normalization predicted by the γ+jets simulation.

As for the inclusive categories, we obtain an alternative estimate from the $W(\to \ell\nu)$+jets-enriched CR to validate the predictions from the γ+jets CR. We require the presence of exactly one tight electron or muon. m_T is required to be between 30 and 100 GeV. The rest of the selection is the same as for the γ+jets CR. The lepton momentum is added vectorially to $\vec{p}_T^{\,\text{miss}}$ to mimic an invisible decay. The $W(\to \ell\nu)$+jets CR yields are extrapolated to the SR via transfer factors calculated from simulation to obtain the alternative $Z \to \nu\bar{\nu}$+jets background estimate. Figure 7 compares the estimates from the γ+jets CR, the $W(\to \ell\nu)$+jets CR, and the MC simulation. The difference between the two alternative estimates based on CRs in data is propagated as a systematic uncertainty.

5.4.3 Multijet background estimation in the boosted categories

The CR enriched in QCD multijet background is defined by inverting the $\Delta\phi_R$ requirement, and requiring antitagged W boson or top quark candidates by inverting the N-subjettiness

Figure 7. Comparison of the estimate of the $Z(\to \nu\nu)$+jets background contribution in the SR extrapolated from the γ+jets CR with the estimate extrapolated from the $W(\to \ell\nu)$+jets CR for the boosted W 4–5 jet (upper left), boosted W 6 jet (upper right) and boosted top (lower) categories in bins of M_R and R^2. The prediction from the uncorrected MC simulation is also shown. The black labels indicate the range in M_R that each set of bins correspond to.

criteria and subjet b tagging for t-tagged jets. Figure 8 shows the distribution in the M_R and R^2 bins for the boosted W 4–5 jet, boosted W 6 jet and boosted top categories. The purity achieved with the selection described above is about 90%. The QCD multijet background is predicted by extrapolating the event yields from this QCD multijet CR to the SRs via transfer factors calculated from simulation.

The effects of inaccuracies in the modeling of the multijet background estimate are taken into account by propagating a systematic uncertainty computed based on the level of disagreement between data and simulation in the b jet multiplicity, N-subjettiness and $\Delta\phi_R$ distributions before applying these selections. The resulting overall systematic uncertainties are 13 and 24% for boosted W and top categories, respectively.

Figure 8. The M_R–R^2 distributions in the QCD multijet CRs of the boosted W 4–5 jet (upper left), boosted W 6 jet (upper right), and boosted top (lower) categories. The ratios of data over MC prediction is shown in the lower panels, where the gray band is the total uncertainty and the dashed band is the statistical uncertainty in the MC prediction.

5.4.4 Validating the background estimation with closure tests in boosted categories

Two validations are performed in CRs similarly to that for the QCD multijet CR but by inverting only one of the two requirements. These validations are intended to verify the reliability of the background estimation method for each requirement individually.

The first validation is performed in a CR that is defined identically to the SR except that we invert the $\Delta\phi_R$ requirement. The comparison between data and predicted back-

ground validates the MC modeling of b tagging, the $\Delta\phi_R$ shape, the extrapolation in the lepton multiplicity, and the accuracy of the efficiency for W boson and top quark tagging. Figure 9 shows the results for the boosted W 4–5 jet, boosted W 6 jet, and boosted top categories. Overall, the estimation agrees with data within uncertainties.

The second validation is performed in a CR defined identically to the SR but requiring antitagged W boson or top quark candidates. This validation is designed to check the modeling of the $\Delta\phi_R$ variable in the QCD multijet and $Z(\nu\overline{\nu})$+jets simulation. The plots in figure 10 show the estimation results compared to data for the boosted W 4–5 jet, boosted W 6 jet, and boosted top categories. Overall, the estimation agrees with data within uncertainties.

6 Systematic uncertainties

Systematic uncertainties considered in this analysis can be broadly categorized into three types: uncertainties from the limited accuracy of calibrations, auxiliary measurements, and theoretical predictions; uncertainties from the data-driven background prediction methodology; and uncertainties specific to the fast simulation prediction of the signal.

Systematic uncertainties of the first type are propagated as shape uncertainties in the signal and background predictions in all event categories. Uncertainties in the trigger and lepton selection efficiency, and in the integrated luminosity [86], primarily affect the total normalization. Uncertainties in the b tagging efficiency affect the relative yields between different b tag categories. Systematic uncertainties in the modeling of the W boson and top quark tagging and mistagging efficiencies affect the yields of the boosted categories. The uncertainties from missing higher-order corrections and the uncertainties in the jet energy and lepton momentum scales affect the shapes of the M_R and R^2 distributions. In Table 3 we summarize these systematic uncertainties and their typical impact on the background and signal predictions.

The second type of systematic uncertainty is related to the background prediction methodology. Statistical uncertainties of the CR data range from 1–20% depending on the M_R and R^2 bin. Systematic uncertainties of the background processes that we are not targeting in each CR contribute at the level of a few percent. Systematic uncertainties related to the accuracy of assumptions made by the background estimation method are estimated through closure tests in different CRs as discussed in section 5. These systematic uncertainties capture the potential modeling inadequacies of the simulation after applying the corrections derived as part of the analysis procedure. They are summarized in table 4.

For the closure tests performed in each N_{jets} bin in the $t\overline{t}$ dilepton and the $Z(\nu\overline{\nu})$+jets dilepton CRs, and the test of the p_T distributions in the loose lepton and τ_h CRs, the uncertainties are applied correlated across all bins. For the checks of the R^2 distributions in each b tag category in the tight lepton and photon CRs, and of the lepton η distributions in the loose lepton and τ_h CRs, the systematic uncertainties are assigned based on the size of the statistical uncertainty in the CRs and are assumed to be uncorrelated from bin to bin.

For the $Z(\nu\overline{\nu})$+jets process, the difference in the correction factors computed in the γ+jets and tight lepton CRs are propagated as a systematic uncertainty. This systematic
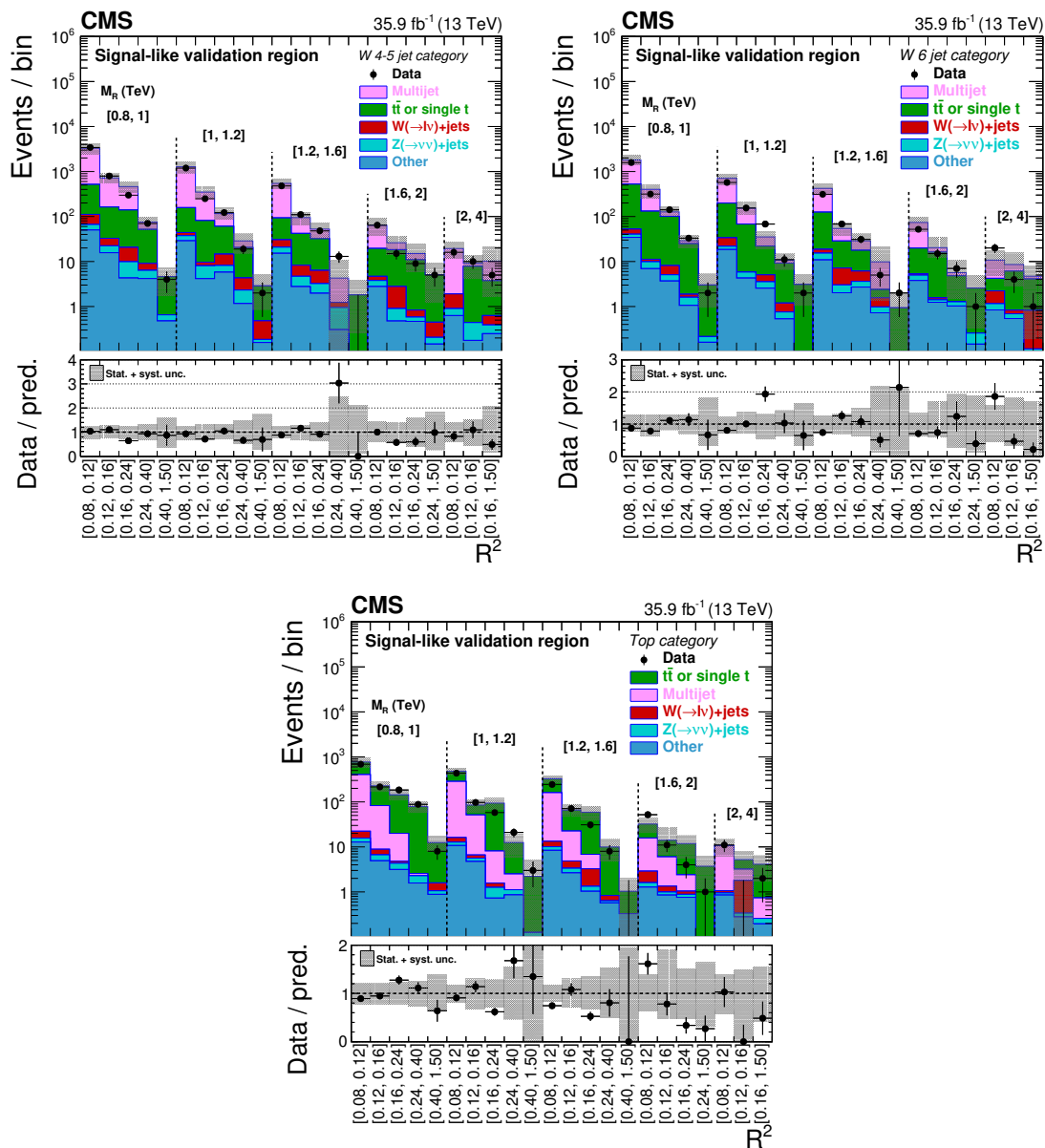
Figure 9. Comparisons between data and the predicted background for the inverted $\Delta\phi_{\mathrm{R}}$ validation region for the boosted W 4–5 jet (upper left), boosted W 6 jet (upper right), and boosted top (lower) categories.

uncertainty estimates the potential differences in the MC mismodeling of the hadronic recoil between the γ+jets process and the $Z(\nu\bar{\nu})$+jets process. These systematic uncertainties range up to 20%.

Finally, there are systematic uncertainties specific to the fast simulation prediction of the signal. These include systematic uncertainties because of possible inaccuracies of the fast simulation in modeling the efficiencies for lepton selection, b tagging, and boosted W boson and top quark tagging. To account for possible mismodeling of the signal accep-

Figure 10. Comparisons between data and the predicted background for the validation region with antitagged W boson or top quark candidates for the boosted W 4–5 jet (upper left), boosted W 6 jet (upper right), and boosted top (lower) categories.

Systematic uncertainty source	On signal and/or bkg	Typical impact of uncertainty on yields (%)
Jet energy scale	Both	6–16
Lepton momentum scale	Both	1
Muon efficiency	Both	1
Electron efficiency	Both	1–2
Trigger efficiency	Both	1
b-tagging efficiency	Both	1–7
b mistagging efficiency	Both	2–20
W/t-tagging efficiency	Both	1–8
W/t-mistagging efficiency	Both	1–3
Higher-order corrections	Both	10–25
Luminosity	Both	2.6
Pileup	Both	1–3
Monte Carlo event count	Both	1–50
Fast simulation corrections	Signal only	1–5
Initial-state radiation	Signal only	4–25

Table 3. Summary of the main instrumental and theoretical systematic uncertainties.

Uncertainty source	Background process	Size (%)
Non-Boosted categories		
1-lepton CR, R^2 closure test	$t\bar{t}$, W+jets	1–95
$t\bar{t}$ 2-lepton closure test	$t\bar{t}$	1–12
Loose lepton p_T closure test	$t\bar{t}$, W+jets	4–50
Loose lepton η closure test	$t\bar{t}$, W+jets	5–40
τ_h p_T closure test	$t\bar{t}$, W+jets	2–43
τ_h η closure test	$t\bar{t}$, W+jets	2–28
γ+jets CR, transfer factor uncertainty and R^2 closure test	$Z(\nu\bar{\nu})$+jets	1–40
DY+jets 2-lepton closure test	$Z(\nu\bar{\nu})$+jets	1–25
QCD multijet transfer factor extrapolation	QCD multijet	30–90
Boosted categories		
QCD multijet modeling	QCD multijet	13–24
DY+jets modeling	$Z(\nu\bar{\nu})$+jets	19–29
$Z(\nu\bar{\nu})$+jets closure test	$Z(\nu\bar{\nu})$+jets	19–98

Table 4. Summary of systematic uncertainties from the background estimation methodology expressed as relative or fractional uncertainties.

tance because of differences in the data and signal MC pileup distributions, we employ a linear fit that extrapolates the acceptance in each analysis bin to the range of pileup values observed in data. Uncertainty in this method is propagated to the signal yield predictions. An additional uncertainty is applied to account for known tendencies for the fast simulation to mismodel the p_T^{miss} in some events. Finally, we propagate an uncertainty in the modeling of the ISR for signal predictions, ranging from 4–25% depending on the number of jets from ISR.

7 Results and interpretation

The observed data yields in the SRs are compatible with the background prediction from SM processes. The results are summarized in the distributions of the M_R and R^2 bins of the SRs. The results for the one-lepton categories are shown in figures 11–14. The main backgrounds are W+jets and $t\bar{t}$ production, with $t\bar{t}$ becoming more dominant with increasing number of b-tagged jets. The three signal scenarios used to interpret the results are also shown.

The results for the zero-lepton boosted categories are shown in figure 15, where $t\bar{t}$ is the dominant background process in all subcategories.

Finally, the results for the zero-lepton non-boosted categories are shown in figures 16–21. The $Z(\nu\bar{\nu})$+jets background is dominant for subcategories with fewer jets and b-tagged jets, while the $t\bar{t}$ background is dominant for subcategories with more jets and b-tagged jets.

We set upper limits on the production cross sections of various SUSY simplified models. We follow the LHC CL_s procedure [87–89] by using the profile likelihood ratio test statistic and the asymptotic formula to evaluate the 95% confidence level (CL) observed and expected limits on the production cross section. Systematic uncertainties are propagated by incorporating nuisance parameters that represent different sources of systematic uncertainty, which are profiled in the maximum likelihood fit [89].

Generally, the best signal sensitivity comes from the Lepton Multijet and Multijet categories, and are dominated by bins with large M_R when the mass splitting between the gluino (or squark) and the LSP is large, and by bins with large R^2 when the mass splitting is small. For signal models that produce many jets, such as gluino pair production with gluinos decaying to two top quarks and the LSP, the Lepton Seven-jet and Seven-jet categories dominate the sensitivity. For signal models with boosted top quarks, such as top squark pair production, the boosted categories contribute significantly to the sensitivity.

First, we consider the scenario of pair produced gluinos decaying to two top quarks and the LSP. The expected and observed limits for such gluino decays are shown as a function of gluino and LSP masses in figure 22. In this simplified model, we exclude gluino masses up to 2.0 TeV for LSP mass below 700 GeV. The limits for gluinos decaying to a top quark and a low mass top squark that subsequently decays to a charm quark and the LSP, is shown in figure 23. For this simplified model, we exclude gluino masses up to 1.9 TeV for LSP mass above 150 and below 950 GeV, extending the previous best limits [35] from the CMS experiment by about 100 GeV in the gluino mass. Finally, we consider pair produced top squarks decaying to the top quark and the LSP. The expected and observed limits are shown in figure 24, and we exclude top squark masses up to 1.14 TeV for LSP mass below 200 GeV, extending the previous best limits [29] from the CMS experiment by about 20 GeV. The dashed blue contour in each exclusion limit plot represents the expected limit obtained using data from the non-boosted categories only. By comparing the expected limits obtained using only the non-boosted categories with the expected limits using all categories, we observe clearly that the boosted categories make an important contribution to the sensitivity for the signal models presented here.
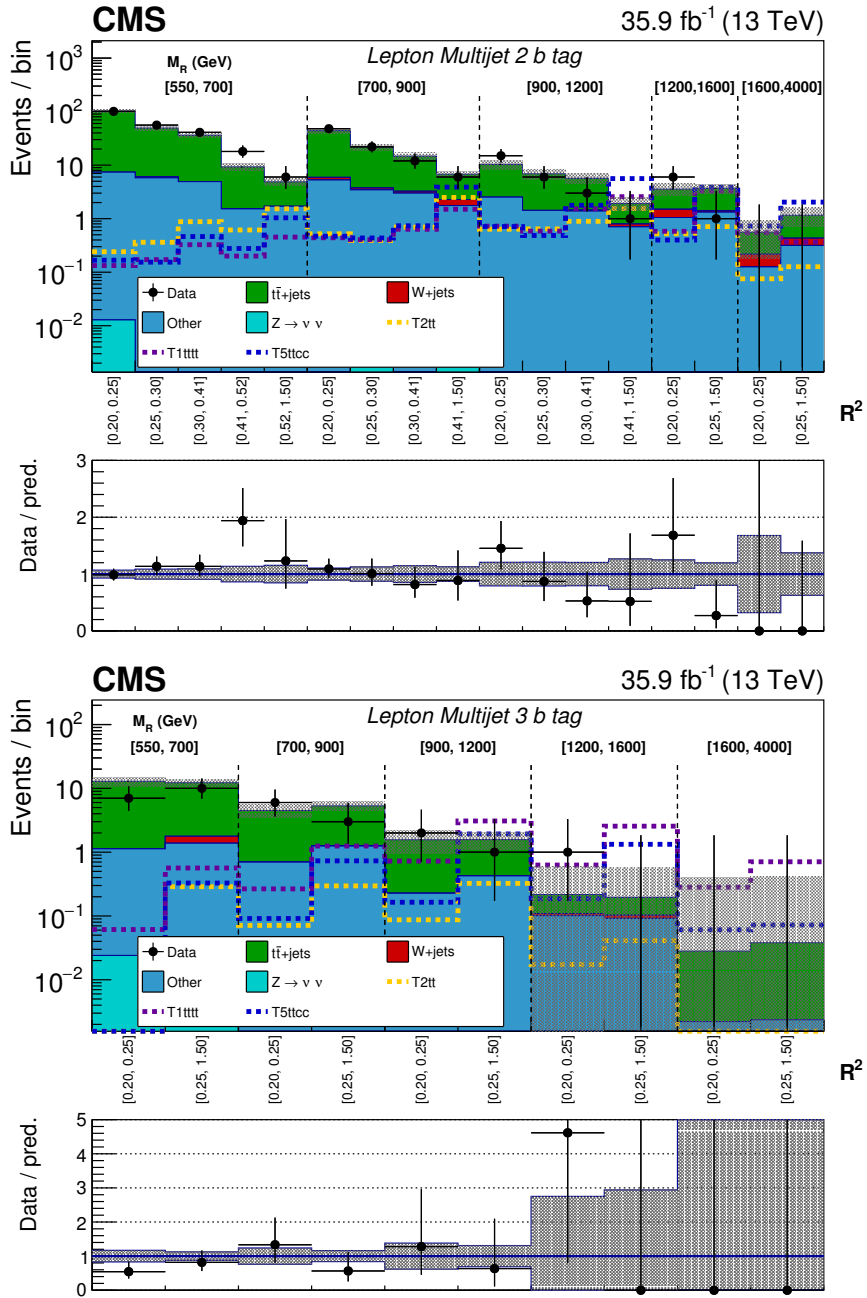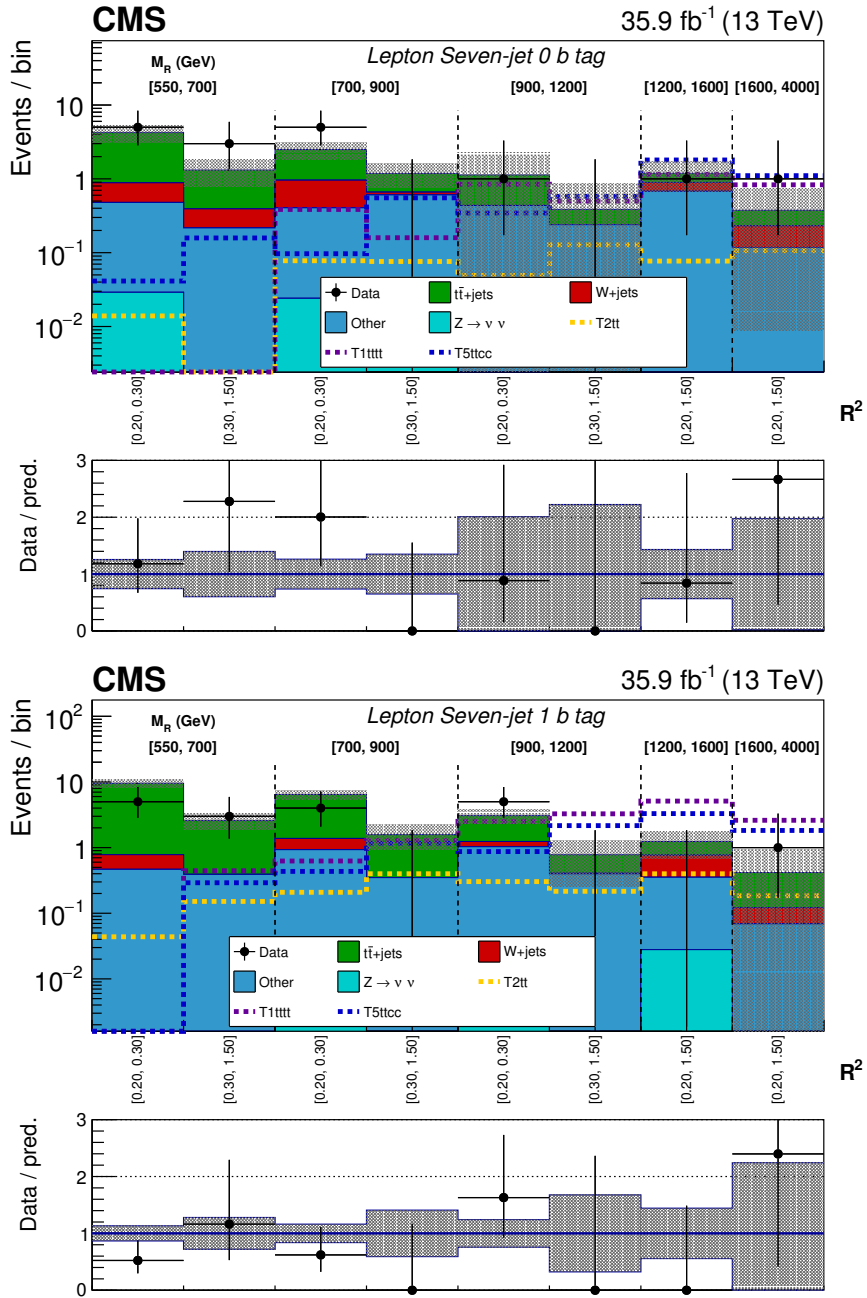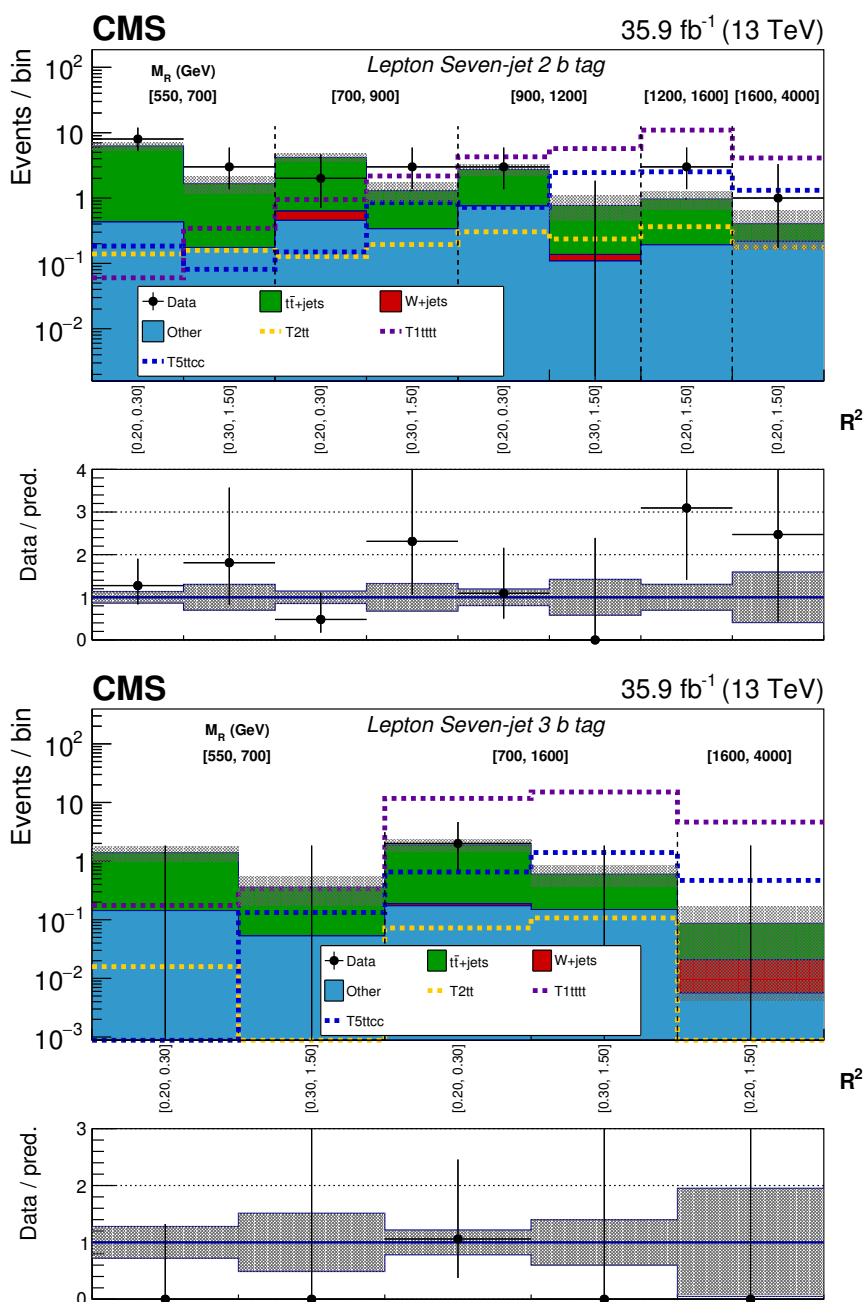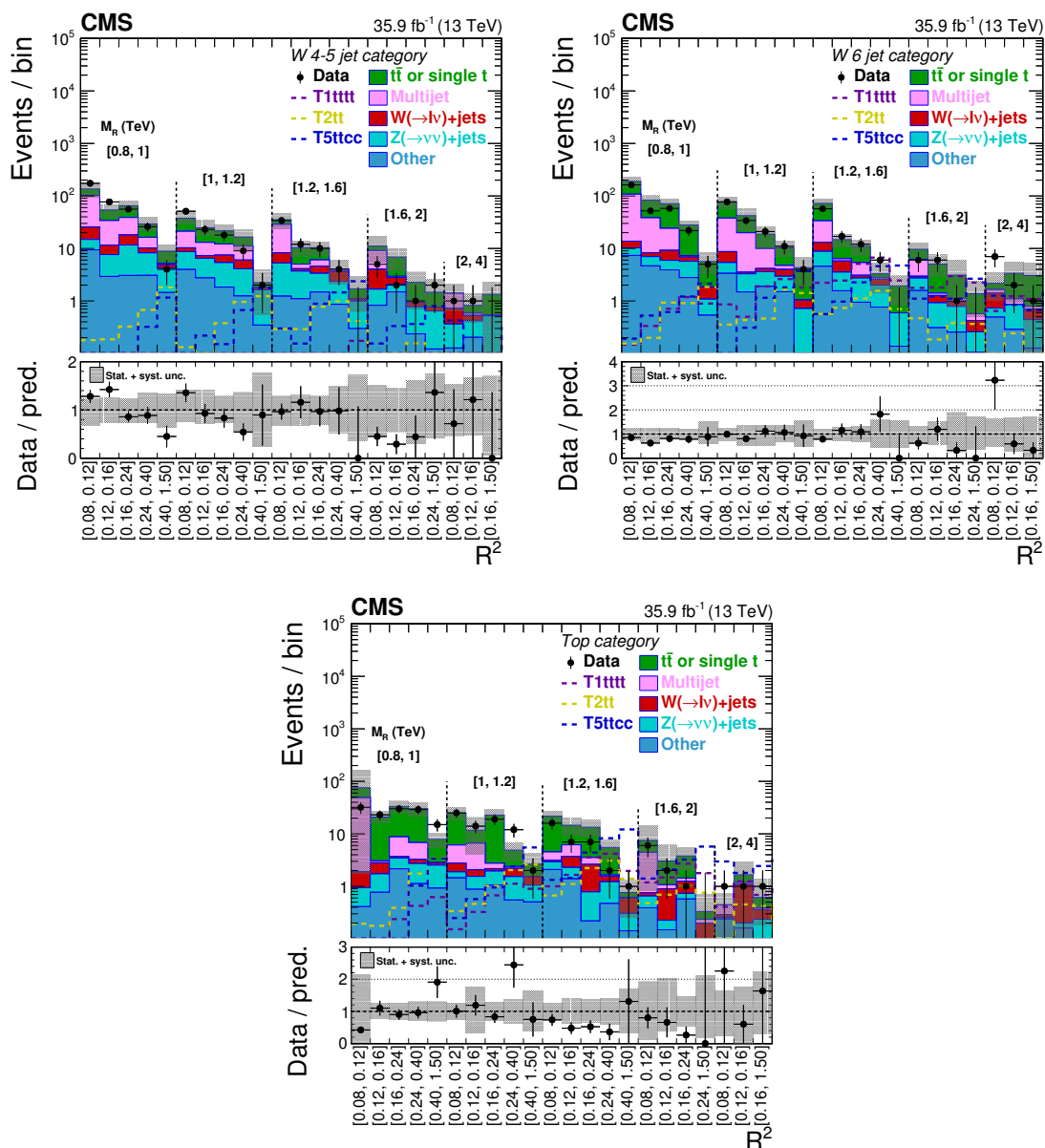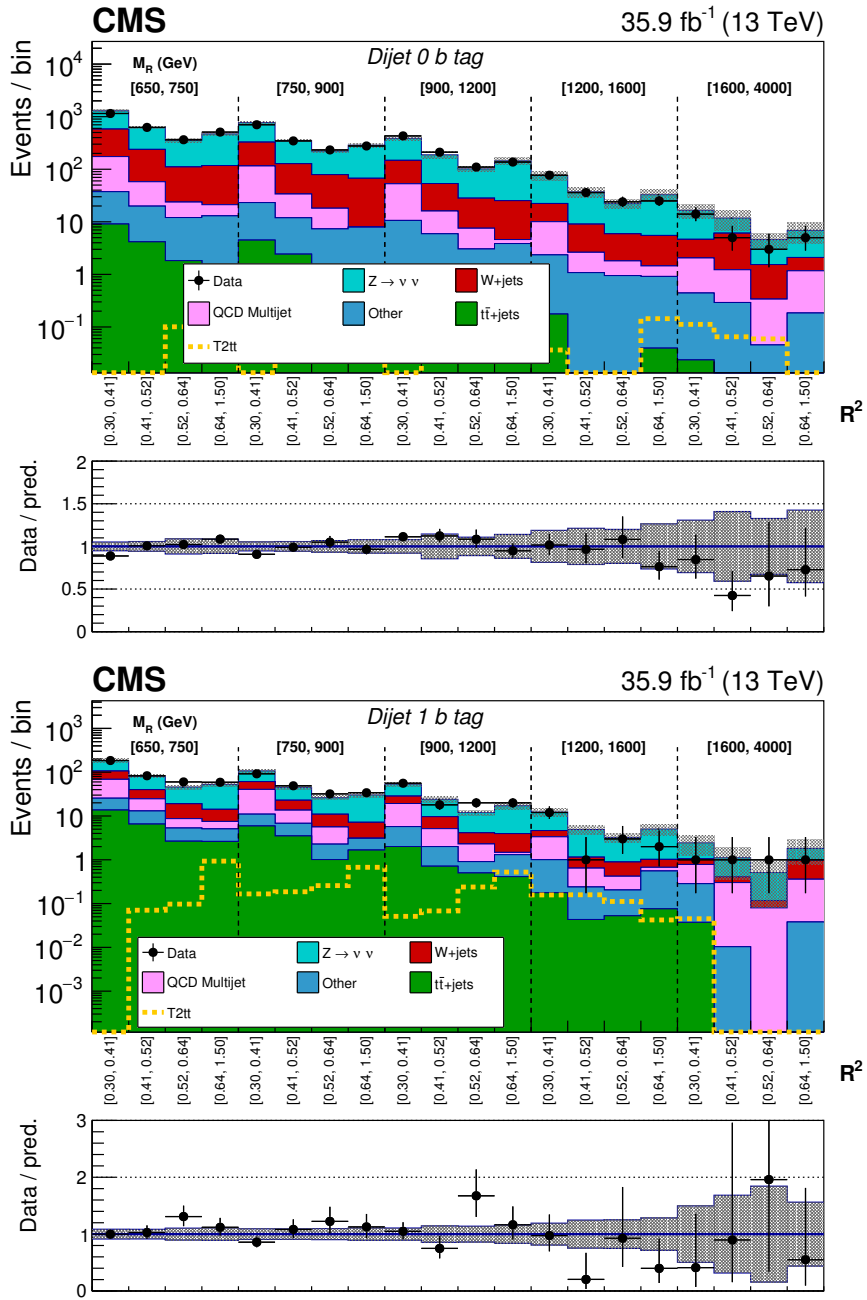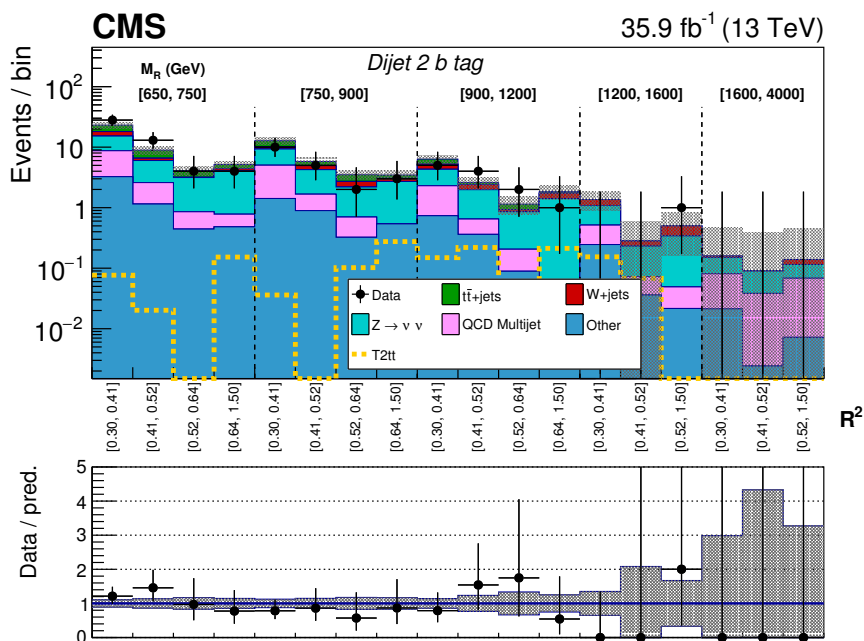
Figure 11. The M_R–R^2 distribution observed in data is shown along with the pre-fit background prediction obtained for the Lepton Multijet event category in the 0 b tag (upper) and 1 b tag (lower) bins. The two-dimensional M_R–R^2 distribution is shown in a one-dimensional representation, with each M_R bin denoted by the dashed lines and labeled above, and each R^2 bin labeled below. The background labeled as "Other" includes single top quark production, diboson production, associated production of a top quark pair and a W or Z boson, and triboson production. The ratio of data to the background prediction is shown on the bottom panel, with the statistical uncertainty expressed through the data point error bars and the systematic uncertainty in the background prediction represented by the shaded region. Signal benchmarks shown are T5ttcc with $m_{\tilde{g}} = 1.4\,\text{TeV}$, $m_{\tilde{t}} = 320\,\text{GeV}$ and $m_{\tilde{\chi}_1^0} = 300\,\text{GeV}$; T1tttt with $m_{\tilde{g}} = 1.4\,\text{TeV}$ and $m_{\tilde{\chi}_1^0} = 300\,\text{GeV}$; and T2tt with $m_{\tilde{t}} = 850\,\text{GeV}$ and $m_{\tilde{\chi}_1^0} = 100\,\text{GeV}$. The diagrams corresponding to these signal models are shown in figure 1.

Figure 12. The M_{R}–R^2 distribution observed in data is shown along with the pre-fit background prediction obtained for the Lepton Multijet event category in the 2 b tag (upper) and 3 or more b tag (lower) bins. Further details of the plots are explained in the caption of figure 11.

Figure 13. The M_R–R^2 distribution observed in data is shown along with the pre-fit background prediction obtained for the Lepton Seven-jet event category in the 0 b tag (upper) and 1 b tag (lower) bins. Further details of the plots are explained in the caption of figure 11.
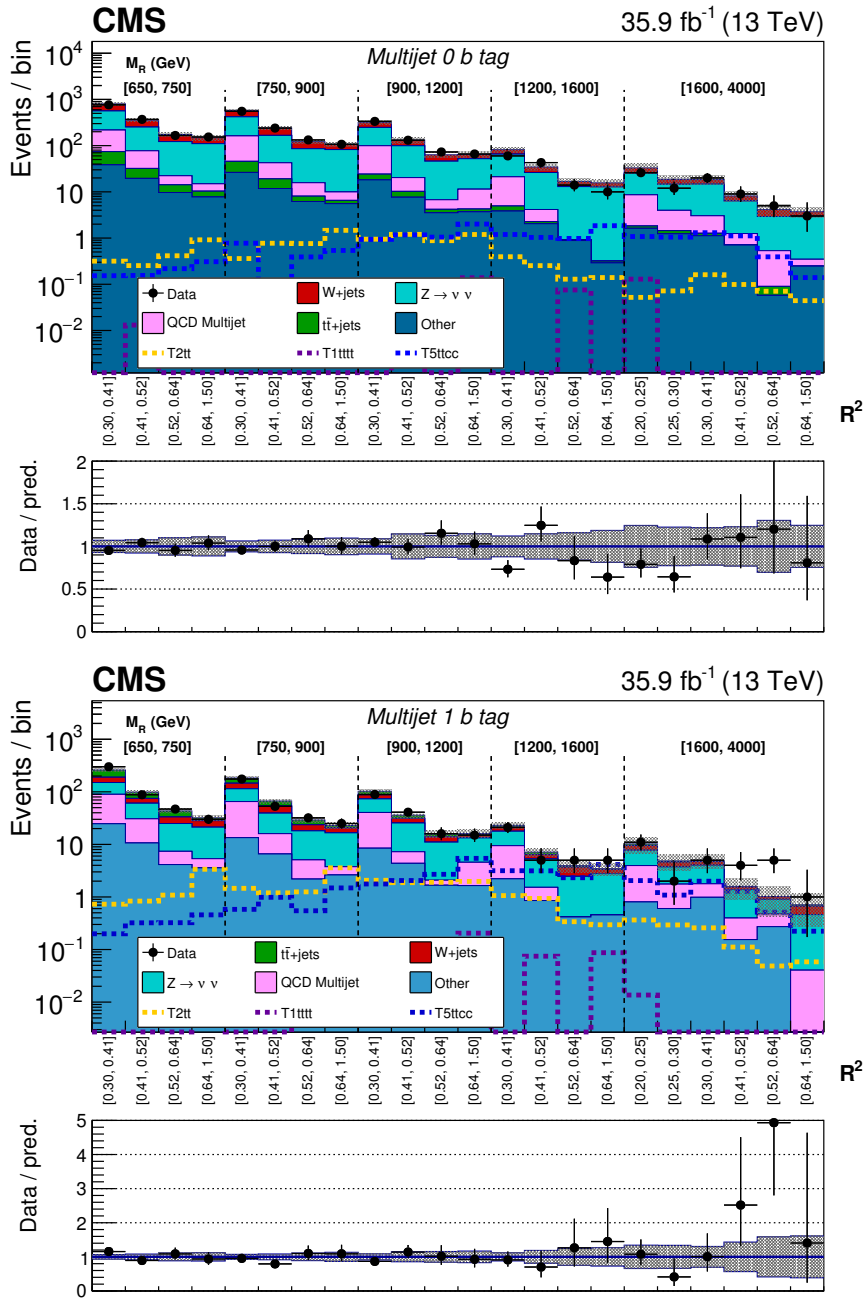
Figure 14. The M_R–R^2 distribution observed in data is shown along with the pre-fit background prediction obtained for the Lepton Seven-jet event category in the 2 b tag (upper) and 3 or more b tag (lower) bins. Further details of the plots are explained in the caption of figure 11.

Figure 15. The M_R–R^2 distribution observed in data is shown along with the pre-fit background prediction obtained for the boosted W 4–5 jet (upper left), boosted W 6 jet (upper right), and Top (lower) categories. Further details of the plots are explained in the caption of figure 11.

8   Summary

We have presented an inclusive search for supersymmetry (SUSY) in events with no more than one lepton, a large multiplicity of energetic jets, and evidence of invisible particles using the razor kinematic variables. To enhance sensitivity to a broad range of signal models, the events are categorized according to the number of leptons, the presence of jets consistent with hadronically decaying W bosons or top quarks, and the number of jets and b-tagged jets. The analysis uses $\sqrt{s} = 13\,\text{TeV}$ proton-proton collision data collected by

Figure 16. The M_R–R^2 distribution observed in data is shown along with the pre-fit background prediction obtained for the Dijet event category in the 0 b tag (upper) and 1 b tag (lower) bins. Further details of the plots are explained in the caption of figure 11.
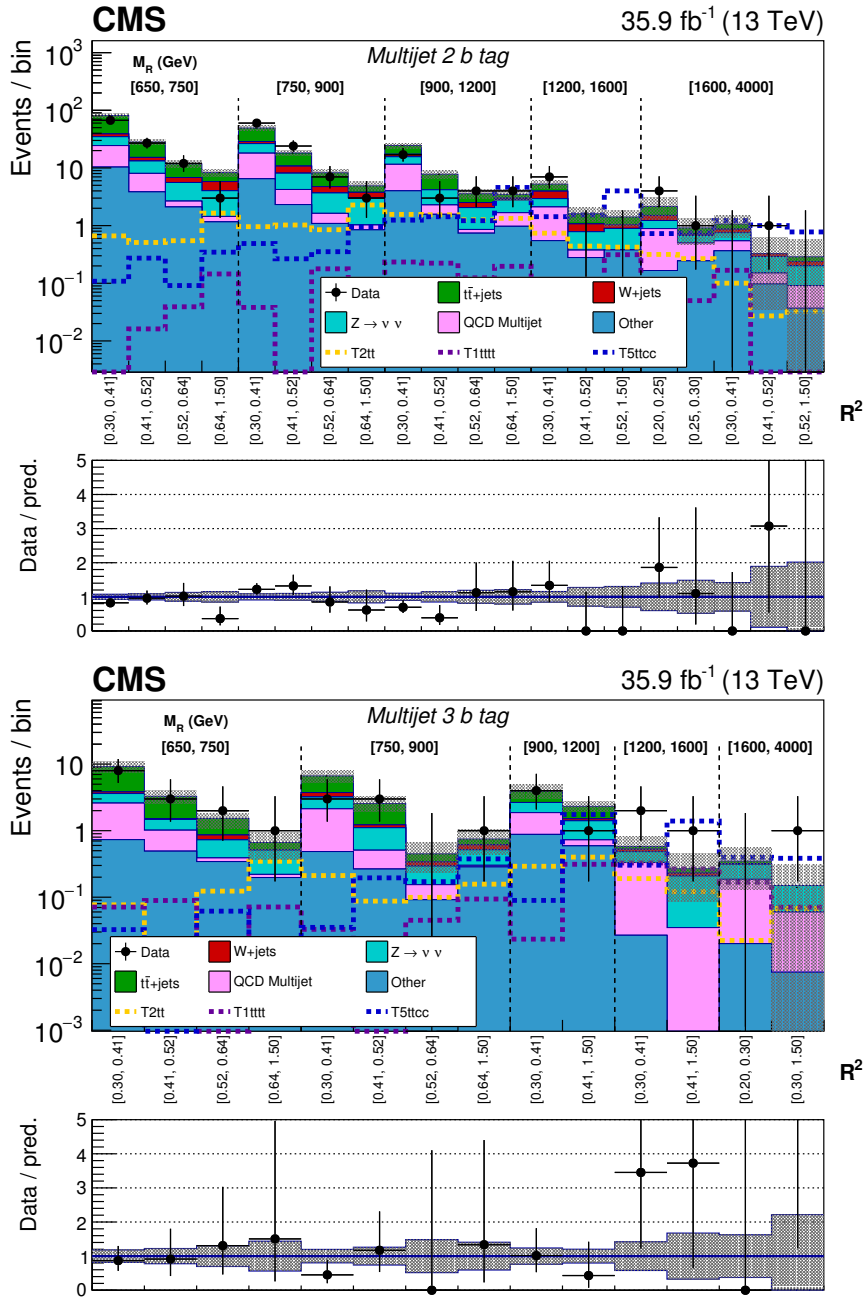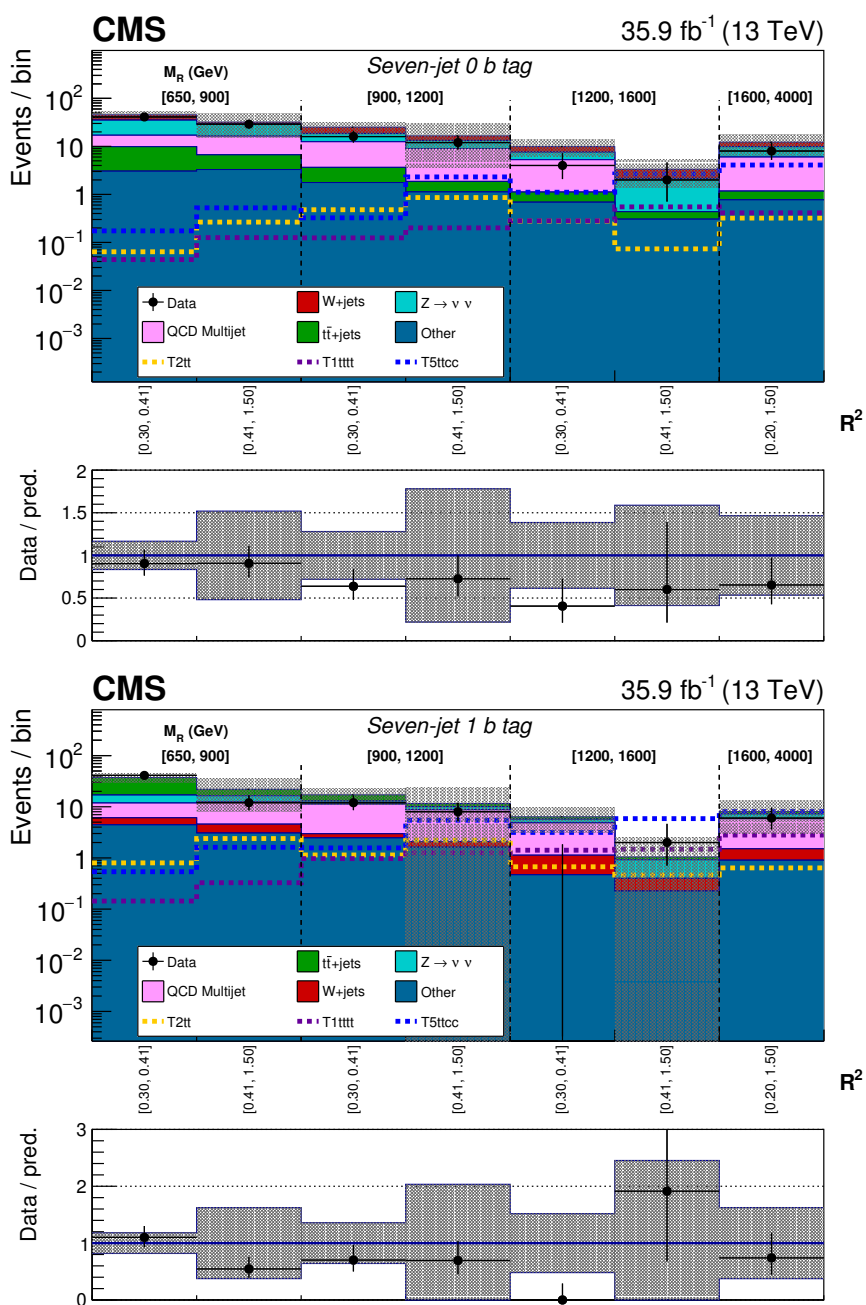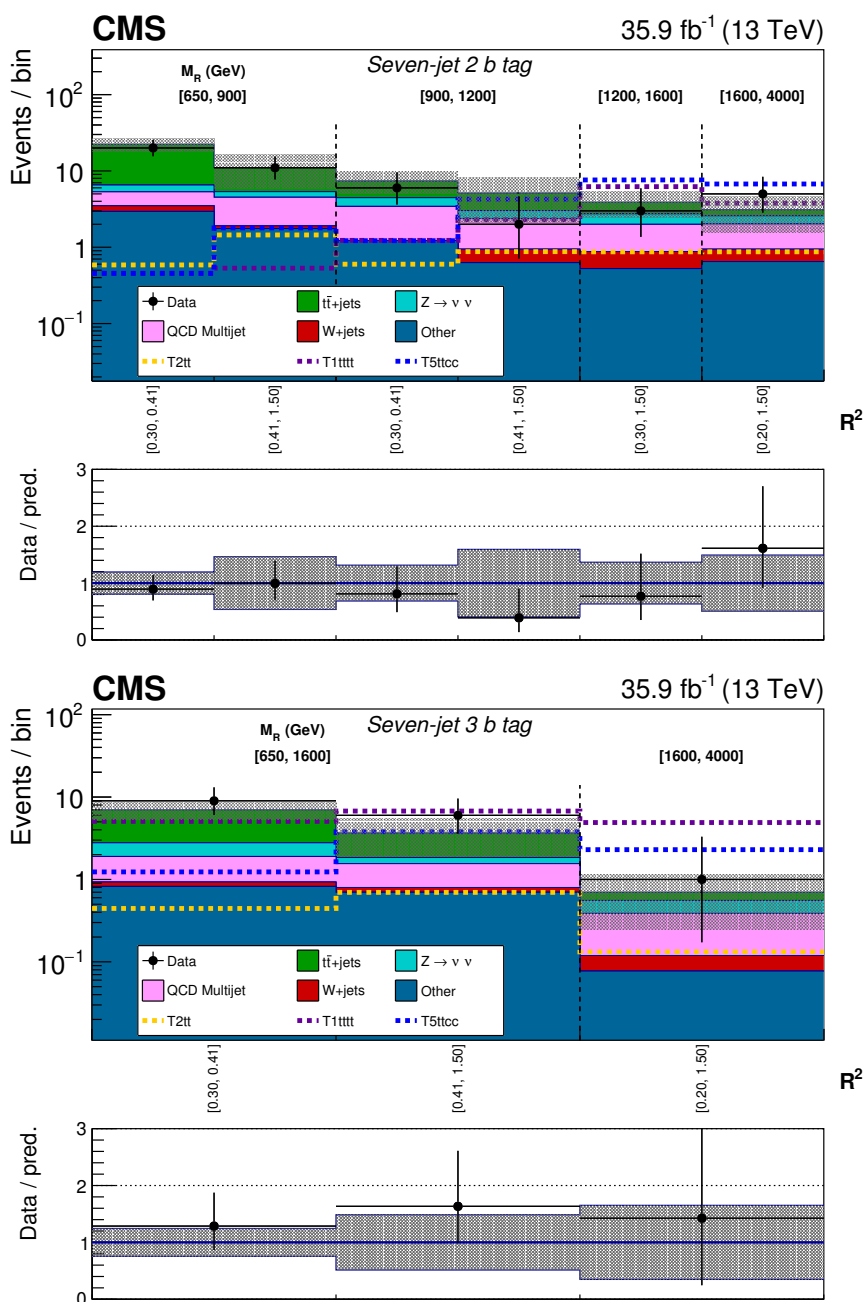
Figure 17. The M_{R}–R^2 distribution observed in data is shown along with the pre-fit background prediction obtained for the Dijet event category in the 2 or more b tag bin. Further details of the plots are explained in the caption of figure 11.

Acknowledgments

Figure 18. The M_R–R^2 distribution observed in data is shown along with the pre-fit background prediction obtained for the Multijet event category in the 0 b tag (upper) and 1 b tag (lower) bins. Further details of the plots are explained in the caption of figure 11.

Figure 19. The M_R–R^2 distribution observed in data is shown along with the pre-fit background prediction obtained for the Multijet event category in the 2 b tag (upper) and 3 or more b tag (lower) bins. Further details of the plots are explained in the caption of figure 11.
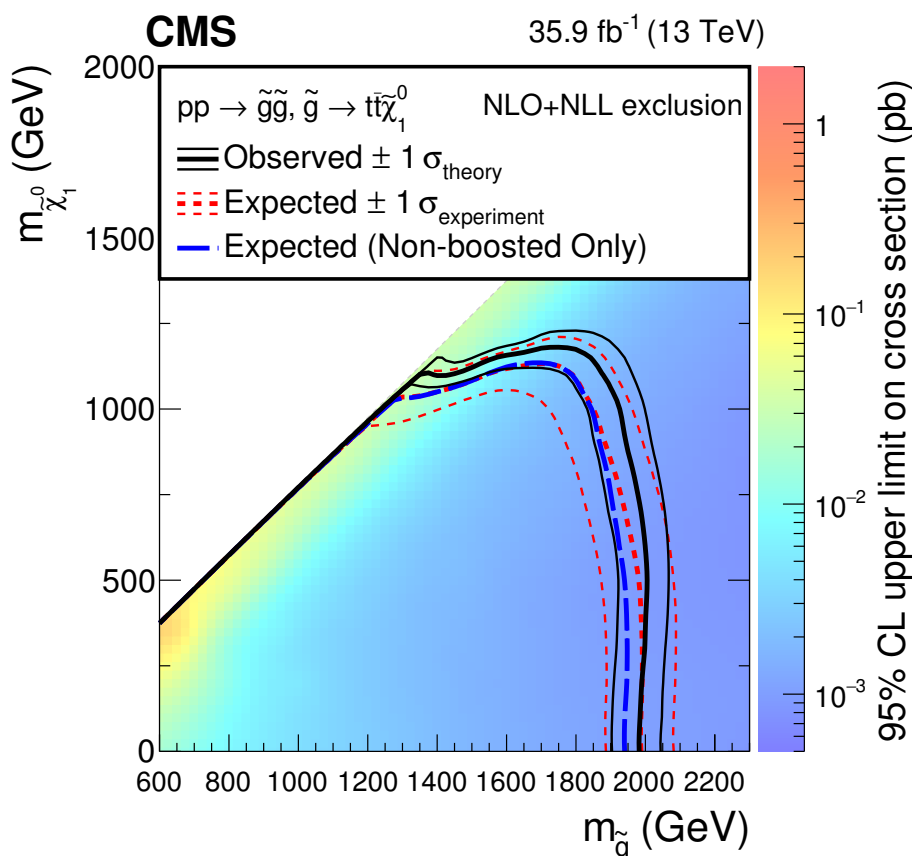
Figure 20. The M_R–R^2 distribution observed in data is shown along with the pre-fit background prediction obtained for the Seven-jet event category in the 0 b tag (upper) and 1 b tag (lower) bins. Further details of the plots are explained in the caption of figure 11.

Figure 21. The M_R–R^2 distribution observed in data is shown along with the pre-fit background prediction obtained for the Seven-jet event category in the 2 b tag (upper) and 3 or more b tag (lower) bins. Further details of the plots are explained in the caption of figure 11.

Figure 22. Expected and observed 95% CL limits on the production cross section for pair-produced gluinos each decaying to the LSP and top quarks. The blue dashed contour represents the expected 95% CL upper limit using data in the non-boosted categories only.
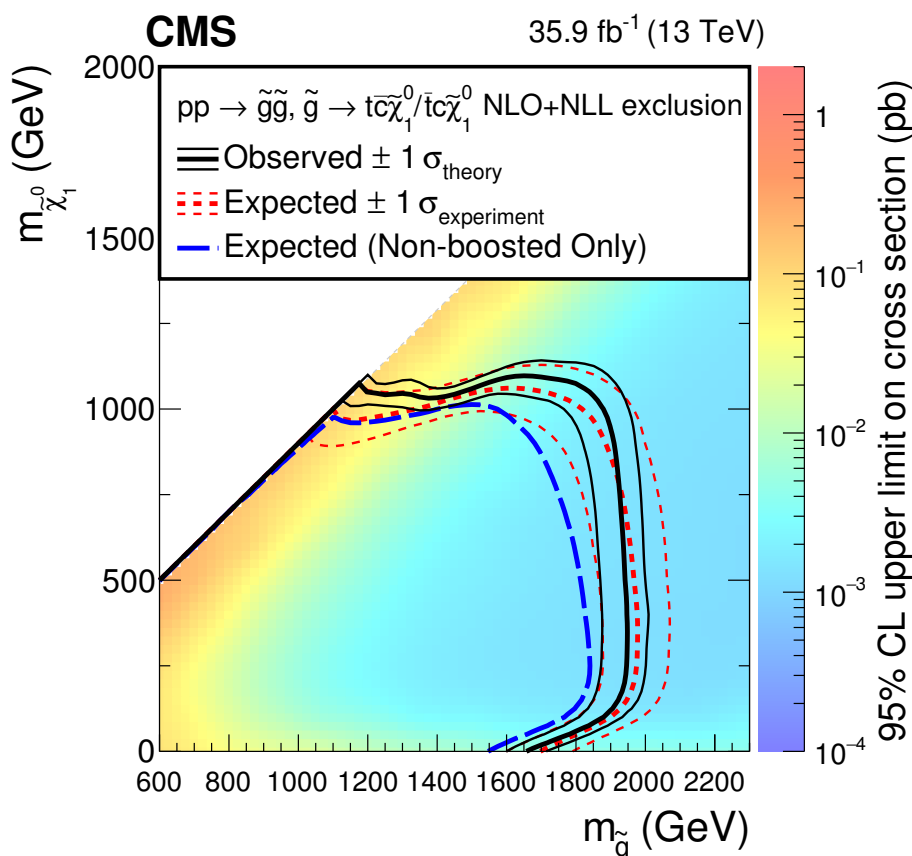
Figure 23. Expected and observed 95% CL limits on the production cross section for pair-produced gluinos each decaying to a top quark and a low mass top squark that subsequently decays to a charm quark and the LSP. The mass splitting $(m_{\tilde{t}} - m_{\tilde{\chi}_1^0})$ is fixed to be 20 GeV. The blue dashed contour represents the expected 95% CL upper limit using data in the non-boosted categories only.

Figure 24. Expected and observed 95% CL limits on the production cross section for pair-produced squarks each decaying to a top quark and the LSP. The blue dashed contour represents the expected 95% CL upper limit using data in the non-boosted categories only. The white diagonal band corresponds to the region $|m_{\tilde{t}} - m_t - m_{\tilde{\chi}_1^0}| < 25\,\text{GeV}$, where the mass difference between the $\tilde{t}$ and the $\tilde{\chi}_1^0$ is very close to the top quark mass. In this region the signal acceptance depends strongly on the $\tilde{\chi}_1^0$ mass and is therefore difficult to model.

References

[1] C. Rogan, *Kinematical variables towards new dynamics at the LHC*, arXiv:1006.2727 [INSPIRE].

[2] CMS collaboration, *Inclusive search for supersymmetry using razor variables in pp collisions at $\sqrt{s} = 13$ TeV*, *Phys. Rev.* **D 95** (2017) 012003 [arXiv:1609.07658] [INSPIRE].

[3] CMS collaboration, *Search for supersymmetry in pp collisions at $\sqrt{s} = 8$ TeV in final states with boosted W bosons and b jets using razor variables*, *Phys. Rev.* **D 93** (2016) 092009 [arXiv:1602.02917] [INSPIRE].

[4] J. Wess and B. Zumino, *Supergauge transformations in four-dimensions*, *Nucl. Phys.* **B 70** (1974) 39 [INSPIRE].

[5] Yu. A. Golfand and E.P. Likhtman, *Extension of the algebra of Poincaré group generators and violation of p invariance*, *JETP Lett.* **13** (1971) 323 [INSPIRE].

[6] D.V. Volkov and V.P. Akulov, *Possible universal neutrino interaction*, *JETP Lett.* **16** (1972) 438 [INSPIRE].

[7] A.H. Chamseddine, R.L. Arnowitt and P. Nath, *Locally supersymmetric grand unification*, *Phys. Rev. Lett.* **49** (1982) 970 [INSPIRE].

[8] G.L. Kane, C.F. Kolda, L. Roszkowski and J.D. Wells, *Study of constrained minimal supersymmetry*, *Phys. Rev.* **D 49** (1994) 6173 [hep-ph/9312272] [INSPIRE].

[9] P. Fayet, *Supergauge invariant extension of the Higgs mechanism and a model for the electron and its neutrino*, *Nucl. Phys.* **B 90** (1975) 104 [INSPIRE].

[10] R. Barbieri, S. Ferrara and C.A. Savoy, *Gauge models with spontaneously broken local supersymmetry*, *Phys. Lett.* **119B** (1982) 343 [INSPIRE].

[11] L.J. Hall, J.D. Lykken and S. Weinberg, *Supergravity as the messenger of supersymmetry breaking*, *Phys. Rev.* **D 27** (1983) 2359 [INSPIRE].

[12] P. Ramond, *Dual theory for free fermions*, *Phys. Rev.* **D 3** (1971) 2415 [INSPIRE].

[13] E. Witten, *Dynamical breaking of supersymmetry*, *Nucl. Phys.* **B 188** (1981) 513 [INSPIRE].

[14] S. Dimopoulos and H. Georgi, *Softly broken supersymmetry and* SU(5), *Nucl. Phys.* **B 193** (1981) 150 [INSPIRE].

[15] M. Dine, W. Fischler and M. Srednicki, *Supersymmetric technicolor*, *Nucl. Phys.* **B 189** (1981) 575 [INSPIRE].

[16] S. Dimopoulos and S. Raby, *Supercolor*, *Nucl. Phys.* **B 192** (1981) 353 [INSPIRE].

[17] N. Sakai, *Naturalness in supersymmetric guts*, *Z. Phys.* **C 11** (1981) 153 [INSPIRE].

[18] R.K. Kaul and P. Majumdar, *Cancellation of quadratically divergent mass corrections in globally supersymmetric spontaneously broken gauge theories*, *Nucl. Phys.* **B 199** (1982) 36 [INSPIRE].

[19] S. Dimopoulos, S. Raby and F. Wilczek, *Supersymmetry and the scale of unification*, *Phys. Rev.* **D 24** (1981) 1681 [INSPIRE].

[20] W.J. Marciano and G. Senjanović, *Predictions of supersymmetric grand unified theories*, *Phys. Rev.* **D 25** (1982) 3092 [INSPIRE].

[21] M.B. Einhorn and D.R.T. Jones, *The weak mixing angle and unification mass in supersymmetric* SU(5), *Nucl. Phys.* **B 196** (1982) 475 [INSPIRE].

[22] L.E. Ibáñez and G.G. Ross, *Low-energy predictions in supersymmetric grand unified theories*, *Phys. Lett.* **105B** (1981) 439 [INSPIRE].

[23] U. Amaldi, W. de Boer and H. Furstenau, *Comparison of grand unified theories with electroweak and strong coupling constants measured at LEP*, *Phys. Lett.* **B 260** (1991) 447 [INSPIRE].

[24] P. Langacker and N. Polonsky, *The strong coupling, unification and recent data*, *Phys. Rev.* **D 52** (1995) 3081 [hep-ph/9503214] [INSPIRE].

[25] J.R. Ellis et al., *Supersymmetric relics from the Big Bang*, *Nucl. Phys.* **B 238** (1984) 453 [INSPIRE].

[26] G. Jungman, M. Kamionkowski and K. Griest, *Supersymmetric dark matter*, *Phys. Rept.* **267** (1996) 195 [hep-ph/9506380] [INSPIRE].

[27] G.R. Farrar and P. Fayet, *Phenomenology of the production, decay and detection of new hadronic states associated with supersymmetry*, *Phys. Lett.* **76B** (1978) 575 [INSPIRE].

[28] CMS collaboration, *Search for natural and split supersymmetry in proton-proton collisions at* $\sqrt{s} = 13$ *TeV in final states with jets and missing transverse momentum*, *JHEP* **05** (2018) 025 [arXiv:1802.02110] [INSPIRE].

[29] CMS collaboration, *Search for top squark pair production in pp collisions at $\sqrt{s} = 13$ TeV using single lepton events*, *JHEP* **10** (2017) 019 [arXiv:1706.04402] [INSPIRE].

[30] CMS collaboration, *Search for new phenomena with the M_{T2} variable in the all-hadronic final state produced in proton–proton collisions at $\sqrt{s} = 13$ TeV*, *Eur. Phys. J.* **C 77** (2017) 710 [arXiv:1705.04650] [INSPIRE].

[31] CMS collaboration, *Search for supersymmetry in pp collisions at $\sqrt{s} = 13$ TeV in the single-lepton final state using the sum of masses of large-radius jets*, *Phys. Rev. Lett.* **119** (2017) 151802 [arXiv:1705.04673] [INSPIRE].

[32] CMS collaboration, *Search for supersymmetry in multijet events with missing transverse momentum in proton-proton collisions at 13 TeV*, *Phys. Rev.* **D 96** (2017) 032003 [arXiv:1704.07781] [INSPIRE].

[33] CMS collaboration, *Search for physics beyond the standard model in events with two leptons of same sign, missing transverse momentum and jets in proton–proton collisions at $\sqrt{s} = 13$ TeV*, *Eur. Phys. J.* **C 77** (2017) 578 [arXiv:1704.07323] [INSPIRE].

[34] CMS collaboration, *Search for supersymmetry in the all-hadronic final state using top quark tagging in pp collisions at $\sqrt{s} = 13$ TeV*, *Phys. Rev.* **D 96** (2017) 012004 [arXiv:1701.01954] [INSPIRE].

[35] CMS collaboration, *Search for supersymmetry in proton-proton collisions at 13 TeV using identified top quarks*, *Phys. Rev.* **D 97** (2018) 012007 [arXiv:1710.11188] [INSPIRE].

[36] CMS collaboration, *Searches for pair production of third-generation squarks in $\sqrt{s} = 13$ TeV pp collisions*, *Eur. Phys. J.* **C 77** (2017) 327 [arXiv:1612.03877] [INSPIRE].

[37] ATLAS collaboration, *Search for a scalar partner of the top quark in the jets plus missing transverse momentum final state at $\sqrt{s} = 13$ TeV with the ATLAS detector*, *JHEP* **12** (2017) 085 [arXiv:1709.04183] [INSPIRE].

[38] ATLAS collaboration, *Search for supersymmetry in events with b-tagged jets and missing transverse momentum in pp collisions at $\sqrt{s} = 13$ TeV with the ATLAS detector*, *JHEP* **11** (2017) 195 [arXiv:1708.09266] [INSPIRE].

[39] ATLAS collaboration, *Search for squarks and gluinos in events with an isolated lepton, jets and missing transverse momentum at $\sqrt{s} = 13$ TeV with the ATLAS detector*, *Phys. Rev.* **D 96** (2017) 112010 [arXiv:1708.08232] [INSPIRE].

[40] ATLAS collaboration, *Search for direct top squark pair production in final states with two leptons in $\sqrt{s} = 13$ TeV pp collisions with the ATLAS detector*, *Eur. Phys. J.* **C 77** (2017) 898 [arXiv:1708.03247] [INSPIRE].

[41] ATLAS collaboration, *Search for new phenomena with large jet multiplicities and missing transverse momentum using large-radius jets and flavour-tagging at ATLAS in 13 TeV pp collisions*, *JHEP* **12** (2017) 034 [arXiv:1708.02794] [INSPIRE].

[42] ATLAS collaboration, *Search for supersymmetry in final states with two same-sign or three leptons and jets using $36\,fb^{-1}$ of $\sqrt{s} = 13$ TeV pp collision data with the ATLAS detector*, *JHEP* **09** (2017) 084 [arXiv:1706.03731] [INSPIRE].

[43] ATLAS collaboration, *Search for new phenomena in a lepton plus high jet multiplicity final state with the ATLAS experiment using $\sqrt{s} = 13$ TeV proton-proton collision data*, *JHEP* **09** (2017) 088 [arXiv:1704.08493] [INSPIRE].

[44] N. Arkani-Hamed et al., *MARMOSET: the path from LHC data to the new standard model via on-shell effective theories*, hep-ph/0703088 [INSPIRE].

[45] J. Alwall, P. Schuster and N. Toro, *Simplified models for a first characterization of new physics at the LHC*, *Phys. Rev.* **D 79** (2009) 075020 [arXiv:0810.3921] [INSPIRE].

[46] J. Alwall, M.-P. Le, M. Lisanti and J.G. Wacker, *Model-independent jets plus missing energy searches*, *Phys. Rev.* **D 79** (2009) 015005 [arXiv:0809.3264] [INSPIRE].

[47] LHC NEW PHYSICS WORKING GROUP collaboration, *Simplified models for LHC new physics searches*, *J. Phys.* **G 39** (2012) 105005 [arXiv:1105.2838] [INSPIRE].

[48] CMS collaboration, *The CMS experiment at the CERN LHC*, 2008 *JINST* **3** S08004 [INSPIRE].

[49] CMS collaboration, *Particle-flow reconstruction and global event description with the CMS detector*, 2017 *JINST* **12** P10003 [arXiv:1706.04965] [INSPIRE].

[50] M. Cacciari, G.P. Salam and G. Soyez, *The anti-k_t jet clustering algorithm*, *JHEP* **04** (2008) 063 [arXiv:0802.1189] [INSPIRE].

[51] M. Cacciari, G.P. Salam and G. Soyez, *FastJet user manual*, *Eur. Phys. J.* **C 72** (2012) 1896 [arXiv:1111.6097] [INSPIRE].

[52] CMS collaboration, *Jet energy scale and resolution in the CMS experiment in pp collisions at 8 TeV*, 2017 *JINST* **12** P02014 [arXiv:1607.03663] [INSPIRE].

[53] CMS collaboration, *Jet algorithms performance in 13 TeV data*, CMS-PAS-JME-16-003 (2016).

[54] CMS collaboration, *Identification of heavy-flavour jets with the CMS detector in pp collisions at 13 TeV*, 2018 *JINST* **13** P05011 [arXiv:1712.07158] [INSPIRE].

[55] J. Thaler and K. Van Tilburg, *Identifying boosted objects with N-subjettiness*, *JHEP* **03** (2011) 015 [arXiv:1011.2268] [INSPIRE].

[56] A.J. Larkoski, S. Marzani, G. Soyez and J. Thaler, *Soft drop*, *JHEP* **05** (2014) 146 [arXiv:1402.2657] [INSPIRE].

[57] CMS collaboration, *Missing transverse energy performance of the CMS detector*, 2011 *JINST* **6** P09001 [arXiv:1106.5048] [INSPIRE].

[58] CMS collaboration, *Performance of the CMS missing transverse momentum reconstruction in pp data at $\sqrt{s} = 8$ TeV*, 2015 *JINST* **10** P02006 [arXiv:1411.0511] [INSPIRE].

[59] CMS Collaboration, *Performance of missing transverse momentum in pp collisions at $\sqrt{s} = 13$ TeV using the CMS detector*, CMS-PAS-JME-17-001 (2017).

[60] CMS collaboration, *Performance of electron reconstruction and selection with the CMS detector in proton-proton collisions at $\sqrt{s} = 8$ TeV*, 2015 *JINST* **10** P06005 [arXiv:1502.02701] [INSPIRE].

[61] CMS collaboration, *Performance of the CMS muon detector and muon reconstruction with proton-proton collisions at $\sqrt{s} = 13$ TeV*, 2018 *JINST* **13** P06015 [arXiv:1804.04528] [INSPIRE].

[62] CMS collaboration, *Reconstruction and identification of τ lepton decays to hadrons and ν_τ at CMS*, 2016 *JINST* **11** P01019 [arXiv:1510.07488] [INSPIRE].

[63] CMS collaboration, *Performance of photon reconstruction and identification with the CMS detector in proton-proton collisions at $\sqrt{s} = 8$ TeV*, 2015 *JINST* **10** P08010 [arXiv:1502.02702] [INSPIRE].

[64] J. Alwall, M. Herquet, F. Maltoni, O. Mattelaer and T. Stelzer, *MadGraph 5: going beyond*, *JHEP* **06** (2011) 128 [arXiv:1106.0522] [INSPIRE].

[65] J. Alwall et al., *The automated computation of tree-level and next-to-leading order differential cross sections and their matching to parton shower simulations*, *JHEP* **07** (2014) 079 [arXiv:1405.0301] [INSPIRE].

[66] T. Sjöstrand et al., *An introduction to PYTHIA 8.2*, *Comput. Phys. Commun.* **191** (2015) 159 [arXiv:1410.3012] [INSPIRE].

[67] S. Hoeche et al., *Matching parton showers and matrix elements*, in the proceedings of *HERA and the LHC: a workshop on the implications of HERA for LHC physics*, March 21–14, Hamburg, Germany (2005), hep-ph/0602031 [INSPIRE].

[68] J. Alwall et al., *Comparative study of various algorithms for the merging of parton showers and matrix elements in hadronic collisions*, *Eur. Phys. J.* **C 53** (2008) 473 [arXiv:0706.2569] [INSPIRE].

[69] CMS collaboration, *Event generator tunes obtained from underlying event and multiparton scattering measurements*, *Eur. Phys. J.* **C 76** (2016) 155 [arXiv:1512.00815] [INSPIRE].

[70] S. Frixione, P. Nason and G. Ridolfi, *A positive-weight next-to-leading-order Monte Carlo for heavy flavour hadroproduction*, *JHEP* **09** (2007) 126 [arXiv:0707.3088] [INSPIRE].

[71] S. Alioli, P. Nason, C. Oleari and E. Re, *NLO single-top production matched with shower in POWHEG: s- and t-channel contributions*, *JHEP* **09** (2009) 111 [*Erratum ibid.* **02** (2010) 011] [arXiv:0907.4076] [INSPIRE].

[72] E. Re, *Single-top Wt-channel production matched with parton showers using the POWHEG method*, *Eur. Phys. J.* **C 71** (2011) 1547 [arXiv:1009.2450] [INSPIRE].

[73] NNPDF collaboration, *Parton distributions for the LHC Run II*, *JHEP* **04** (2015) 040 [arXiv:1410.8849] [INSPIRE].

[74] GEANT4 collaboration, *GEANT4: a simulation toolkit*, *Nucl. Instrum. Meth.* **A 506** (2003) 250 [INSPIRE].

[75] CMS collaboration, *The fast simulation of the CMS detector at LHC*, *J. Phys. Conf. Ser.* **331** (2011) 032049.

[76] W. Beenakker, R. Hopker, M. Spira and P.M. Zerwas, *Squark and gluino production at hadron colliders*, *Nucl. Phys.* **B 492** (1997) 51 [hep-ph/9610490] [INSPIRE].

[77] A. Kulesza and L. Motyka, *Threshold resummation for squark-antisquark and gluino-pair production at the LHC*, *Phys. Rev. Lett.* **102** (2009) 111802 [arXiv:0807.2405] [INSPIRE].

[78] A. Kulesza and L. Motyka, *Soft gluon resummation for the production of gluino-gluino and squark-antisquark pairs at the LHC*, *Phys. Rev.* **D 80** (2009) 095004 [arXiv:0905.4749] [INSPIRE].

[79] W. Beenakker et al., *Soft-gluon resummation for squark and gluino hadroproduction*, *JHEP* **12** (2009) 041 [arXiv:0909.4418] [INSPIRE].

[80] W. Beenakker et al., *Squark and Gluino Hadroproduction*, *Int. J. Mod. Phys.* **A 26** (2011) 2637 [arXiv:1105.1110] [INSPIRE].

[81] C. Borschensky et al., *Squark and gluino production cross sections in pp collisions at* $\sqrt{s}$ = 13, 14, 33 *and* 100 *TeV*, *Eur. Phys. J.* **C 74** (2014) 3174 [arXiv:1407.5066] [INSPIRE].

[82] CMS collaboration, *Inclusive search for squarks and gluinos in pp collisions at* $\sqrt{s}$ = 7 *TeV*, *Phys. Rev.* **D 85** (2012) 012004 [arXiv:1107.1279] [INSPIRE].

[83] CMS collaboration, *Comparison of the* Z/γ^* + *jets to* γ + *jets cross sections in pp collisions at* $\sqrt{s}$ = 8 *TeV*, *JHEP* **10** (2015) 128 [*Erratum ibid.* **04** (2016) 010] [arXiv:1505.06520] [INSPIRE].

[84] S.D. Ellis, R. Kleiss and W.J. Stirling, *W's, Z's and jets*, *Phys. Lett.* **154B** (1985) 435 [INSPIRE].

[85] F.A. Berends et al., *Multi-jet production in W, Z events at* $p\bar{p}$ *colliders*, *Phys. Lett.* **B 224** (1989) 237 [INSPIRE].

[86] CMS collaboration, *CMS luminosity measurements for the 2016 data taking period*, CMS-PAS-LUM-17-001 (2017).

[87] A.L. Read, *Presentation of search results: the* CL_s *technique*, *J. Phys.* **G 28** (2002) 2693 [INSPIRE].

[88] T. Junk, *Confidence level computation for combining searches with small statistics*, *Nucl. Instrum. Meth.* **A 434** (1999) 435 [hep-ex/9902006] [INSPIRE].

[89] ATLAS, CMS collaborations and The LHC Higgs Combination Group, *Procedure for the LHC Higgs boson search combination in Summer 2011*, CMS-NOTE-2011-005 (2011).

The CMS collaboration

Yerevan Physics Institute, Yerevan, Armenia

A.M. Sirunyan, A. Tumasyan

Institut für Hochenergiephysik, Wien, Austria

W. Adam, F. Ambrogi, E. Asilar, T. Bergauer, J. Brandstetter, M. Dragicevic, J. Erö, A. Escalante Del Valle, M. Flechl, R. Frühwirth[1], V.M. Ghete, J. Hrubec, M. Jeitler[1], N. Krammer, I. Krätschmer, D. Liko, T. Madlener, I. Mikulec, N. Rad, H. Rohringer, J. Schieck[1], R. Schöfbeck, M. Spanring, D. Spitzbart, W. Waltenberger, J. Wittmann, C.-E. Wulz[1], M. Zarucki

Institute for Nuclear Problems, Minsk, Belarus

V. Chekhovsky, V. Mossolov, J. Suarez Gonzalez

Universiteit Antwerpen, Antwerpen, Belgium

E.A. De Wolf, D. Di Croce, X. Janssen, J. Lauwers, A. Lelek, M. Pieters, H. Van Haevermaet, P. Van Mechelen, N. Van Remortel

Vrije Universiteit Brussel, Brussel, Belgium

S. Abu Zeid, F. Blekman, J. D'Hondt, J. De Clercq, K. Deroover, G. Flouris, D. Lontkovskyi, S. Lowette, I. Marchesini, S. Moortgat, L. Moreels, Q. Python, K. Skovpen, S. Tavernier, W. Van Doninck, P. Van Mulders, I. Van Parijs

Université Libre de Bruxelles, Bruxelles, Belgium

D. Beghin, B. Bilin, H. Brun, B. Clerbaux, G. De Lentdecker, H. Delannoy, B. Dorney, G. Fasanella, L. Favart, A. Grebenyuk, A.K. Kalsi, T. Lenzi, J. Luetic, N. Postiau, E. Starling, L. Thomas, C. Vander Velde, P. Vanlaer, D. Vannerom, Q. Wang

Ghent University, Ghent, Belgium

T. Cornelis, D. Dobur, A. Fagot, M. Gul, I. Khvastunov[2], D. Poyraz, C. Roskas, D. Trocino, M. Tytgat, W. Verbeke, B. Vermassen, M. Vit, N. Zaganidis

Université Catholique de Louvain, Louvain-la-Neuve, Belgium

H. Bakhshiansohi, O. Bondu, G. Bruno, C. Caputo, P. David, C. Delaere, M. Delcourt, A. Giammanco, G. Krintiras, V. Lemaitre, A. Magitteri, K. Piotrzkowski, A. Saggio, M. Vidal Marono, P. Vischia, J. Zobec

Centro Brasileiro de Pesquisas Fisicas, Rio de Janeiro, Brazil

F.L. Alves, G.A. Alves, G. Correia Silva, C. Hensel, A. Moraes, M.E. Pol, P. Rebello Teles

Universidade do Estado do Rio de Janeiro, Rio de Janeiro, Brazil

E. Belchior Batista Das Chagas, W. Carvalho, J. Chinellato[3], E. Coelho, E.M. Da Costa, G.G. Da Silveira[4], D. De Jesus Damiao, C. De Oliveira Martins, S. Fonseca De Souza, H. Malbouisson, D. Matos Figueiredo, M. Melo De Almeida, C. Mora Herrera, L. Mundim, H. Nogima, W.L. Prado Da Silva, L.J. Sanchez Rosas, A. Santoro, A. Sznajder, M. Thiel, E.J. Tonelli Manganote[3], F. Torres Da Silva De Araujo, A. Vilela Pereira

Universidade Estadual Paulista[a], Universidade Federal do ABC[b], São Paulo, Brazil

S. Ahuja[a], C.A. Bernardes[a], L. Calligaris[a], T.R. Fernandez Perez Tomei[a], E.M. Gregores[b], P.G. Mercadante[b], S.F. Novaes[a], SandraS. Padula[a]

Institute for Nuclear Research and Nuclear Energy, Bulgarian Academy of Sciences, Sofia, Bulgaria

A. Aleksandrov, R. Hadjiiska, P. Iaydjiev, A. Marinov, M. Misheva, M. Rodozov, M. Shopova, G. Sultanov

University of Sofia, Sofia, Bulgaria

A. Dimitrov, L. Litov, B. Pavlov, P. Petkov

Beihang University, Beijing, China

W. Fang[5], X. Gao[5], L. Yuan

Institute of High Energy Physics, Beijing, China

M. Ahmad, J.G. Bian, G.M. Chen, H.S. Chen, M. Chen, Y. Chen, C.H. Jiang, D. Leggat, H. Liao, Z. Liu, S.M. Shaheen[6], A. Spiezia, J. Tao, E. Yazgan, H. Zhang, S. Zhang[6], J. Zhao

State Key Laboratory of Nuclear Physics and Technology, Peking University, Beijing, China

Y. Ban, G. Chen, A. Levin, J. Li, L. Li, Q. Li, Y. Mao, S.J. Qian, D. Wang

Tsinghua University, Beijing, China

Y. Wang

Universidad de Los Andes, Bogota, Colombia

C. Avila, A. Cabrera, C.A. Carrillo Montoya, L.F. Chaparro Sierra, C. Florez, C.F. González Hernández, M.A. Segura Delgado

University of Split, Faculty of Electrical Engineering, Mechanical Engineering and Naval Architecture, Split, Croatia

B. Courbon, N. Godinovic, D. Lelas, I. Puljak, T. Sculac

University of Split, Faculty of Science, Split, Croatia

Z. Antunovic, M. Kovac

Institute Rudjer Boskovic, Zagreb, Croatia

V. Brigljevic, D. Ferencek, K. Kadija, B. Mesic, M. Roguljic, A. Starodumov[7], T. Susa

University of Cyprus, Nicosia, Cyprus

M.W. Ather, A. Attikis, M. Kolosova, G. Mavromanolakis, J. Mousa, C. Nicolaou, F. Ptochos, P.A. Razis, H. Rykaczewski

Charles University, Prague, Czech Republic

M. Finger[8], M. Finger Jr.[8]

Escuela Politecnica Nacional, Quito, Ecuador

E. Ayala

Universidad San Francisco de Quito, Quito, Ecuador

E. Carrera Jarrin

Academy of Scientific Research and Technology of the Arab Republic of Egypt, Egyptian Network of High Energy Physics, Cairo, Egypt

Y. Assran[9,10], S. Elgammal[10], S. Khalil[11]

National Institute of Chemical Physics and Biophysics, Tallinn, Estonia

S. Bhowmik, A. Carvalho Antunes De Oliveira, R.K. Dewanjee, K. Ehataht, M. Kadastik, M. Raidal, C. Veelken

Department of Physics, University of Helsinki, Helsinki, Finland

P. Eerola, H. Kirschenmann, J. Pekkanen, M. Voutilainen

Helsinki Institute of Physics, Helsinki, Finland

J. Havukainen, J.K. Heikkilä, T. Järvinen, V. Karimäki, R. Kinnunen, T. Lampén, K. Lassila-Perini, S. Laurila, S. Lehti, T. Lindén, P. Luukka, T. Mäenpää, H. Siikonen, E. Tuominen, J. Tuominiemi

Lappeenranta University of Technology, Lappeenranta, Finland

T. Tuuva

IRFU, CEA, Université Paris-Saclay, Gif-sur-Yvette, France

M. Besancon, F. Couderc, M. Dejardin, D. Denegri, J.L. Faure, F. Ferri, S. Ganjour, A. Givernaud, P. Gras, G. Hamel de Monchenault, P. Jarry, C. Leloup, E. Locci, J. Malcles, G. Negro, J. Rander, A. Rosowsky, M.Ö. Sahin, M. Titov

Laboratoire Leprince-Ringuet, Ecole polytechnique, CNRS/IN2P3, Université Paris-Saclay, Palaiseau, France

A. Abdulsalam[12], C. Amendola, I. Antropov, F. Beaudette, P. Busson, C. Charlot, R. Granier de Cassagnac, I. Kucher, A. Lobanov, J. Martin Blanco, C. Martin Perez, M. Nguyen, C. Ochando, G. Ortona, P. Paganini, J. Rembser, R. Salerno, J.B. Sauvan, Y. Sirois, A.G. Stahl Leiton, A. Zabi, A. Zghiche

Université de Strasbourg, CNRS, IPHC UMR 7178, Strasbourg, France

J.-L. Agram[13], J. Andrea, D. Bloch, G. Bourgatte, J.-M. Brom, E.C. Chabert, V. Cherepanov, C. Collard, E. Conte[13], J.-C. Fontaine[13], D. Gelé, U. Goerlach, M. Jansová, A.-C. Le Bihan, N. Tonon, P. Van Hove

Centre de Calcul de l'Institut National de Physique Nucleaire et de Physique des Particules, CNRS/IN2P3, Villeurbanne, France

S. Gadrat

Université de Lyon, Université Claude Bernard Lyon 1, CNRS-IN2P3, Institut de Physique Nucléaire de Lyon, Villeurbanne, France

S. Beauceron, C. Bernet, G. Boudoul, N. Chanon, R. Chierici, D. Contardo, P. Depasse, H. El Mamouni, J. Fay, L. Finco, S. Gascon, M. Gouzevitch, G. Grenier, B. Ille, F. Lagarde, I.B. Laktineh, H. Lattaud, M. Lethuillier, L. Mirabito, S. Perries, A. Popov[14], V. Sordini, G. Touquet, M. Vander Donckt, S. Viret

Georgian Technical University, Tbilisi, Georgia

A. Khvedelidze[8]

Tbilisi State University, Tbilisi, Georgia

Z. Tsamalaidze[8]

RWTH Aachen University, I. Physikalisches Institut, Aachen, Germany

C. Autermann, L. Feld, M.K. Kiesel, K. Klein, M. Lipinski, M. Preuten, M.P. Rauch, C. Schomakers, J. Schulz, M. Teroerde, B. Wittmer

RWTH Aachen University, III. Physikalisches Institut A, Aachen, Germany

A. Albert, M. Erdmann, S. Erdweg, T. Esch, R. Fischer, S. Ghosh, A. Güth, T. Hebbeker, C. Heidemann, K. Hoepfner, H. Keller, L. Mastrolorenzo, M. Merschmeyer, A. Meyer, P. Millet, S. Mukherjee, T. Pook, M. Radziej, H. Reithler, M. Rieger, A. Schmidt, D. Teyssier, S. Thüer

RWTH Aachen University, III. Physikalisches Institut B, Aachen, Germany

G. Flügge, O. Hlushchenko, T. Kress, T. Müller, A. Nehrkorn, A. Nowack, C. Pistone, O. Pooth, D. Roy, H. Sert, A. Stahl[15]

Deutsches Elektronen-Synchrotron, Hamburg, Germany

M. Aldaya Martin, T. Arndt, C. Asawatangtrakuldee, I. Babounikau, K. Beernaert, O. Behnke, U. Behrens, A. Bermúdez Martínez, D. Bertsche, A.A. Bin Anuar, K. Borras[16], V. Botta, A. Campbell, P. Connor, C. Contreras-Campana, V. Danilov, A. De Wit, M.M. Defranchis, C. Diez Pardos, D. Domínguez Damiani, G. Eckerlin, T. Eichhorn, A. Elwood, E. Eren, E. Gallo[17], A. Geiser, J.M. Grados Luyando, A. Grohsjean, M. Guthoff, M. Haranko, A. Harb, H. Jung, M. Kasemann, J. Keaveney, C. Kleinwort, J. Knolle, D. Krücker, W. Lange, T. Lenz, J. Leonard, K. Lipka, W. Lohmann[18], R. Mankel, I.-A. Melzer-Pellmann, A.B. Meyer, M. Meyer, M. Missiroli, G. Mittag, J. Mnich, V. Myronenko, S.K. Pflitsch, D. Pitzl, A. Raspereza, A. Saibel, M. Savitskyi, P. Saxena, P. Schütze, C. Schwanenberger, R. Shevchenko, A. Singh, H. Tholen, O. Turkot, A. Vagnerini, M. Van De Klundert, G.P. Van Onsem, R. Walsh, Y. Wen, K. Wichmann, C. Wissing, O. Zenaiev

University of Hamburg, Hamburg, Germany

R. Aggleton, S. Bein, L. Benato, A. Benecke, T. Dreyer, A. Ebrahimi, E. Garutti, D. Gonzalez, P. Gunnellini, J. Haller, A. Hinzmann, A. Karavdina, G. Kasieczka, R. Klanner, R. Kogler, N. Kovalchuk, S. Kurz, V. Kutzner, J. Lange, D. Marconi, J. Multhaup, M. Niedziela, C.E.N. Niemeyer, D. Nowatschin, A. Perieanu, A. Reimers, O. Rieger, C. Scharf, P. Schleper, S. Schumann, J. Schwandt, J. Sonneveld, H. Stadie, G. Steinbrück, F.M. Stober, M. Stöver, B. Vormwald, I. Zoi

Karlsruher Institut fuer Technologie, Karlsruhe, Germany

M. Akbiyik, C. Barth, M. Baselga, S. Baur, E. Butz, R. Caspart, T. Chwalek, F. Colombo, W. De Boer, A. Dierlamm, K. El Morabit, N. Faltermann, B. Freund, M. Giffels, M.A. Harrendorf, F. Hartmann[15], S.M. Heindl, U. Husemann, I. Katkov[14], S. Kudella, S. Mitra, M.U. Mozer, Th. Müller, M. Musich, M. Plagge, G. Quast, K. Rabbertz,

M. Schröder, I. Shvetsov, H.J. Simonis, R. Ulrich, S. Wayand, M. Weber, T. Weiler, C. Wöhrmann, R. Wolf

Institute of Nuclear and Particle Physics (INPP), NCSR Demokritos, Aghia Paraskevi, Greece

G. Anagnostou, G. Daskalakis, T. Geralis, A. Kyriakis, D. Loukas, G. Paspalaki

National and Kapodistrian University of Athens, Athens, Greece

A. Agapitos, G. Karathanasis, P. Kontaxakis, A. Panagiotou, I. Papavergou, N. Saoulidou, K. Vellidis

National Technical University of Athens, Athens, Greece

K. Kousouris, I. Papakrivopoulos, G. Tsipolitis

University of Ioánnina, Ioánnina, Greece

I. Evangelou, C. Foudas, P. Gianneios, P. Katsoulis, P. Kokkas, S. Mallios, N. Manthos, I. Papadopoulos, E. Paradas, J. Strologas, F.A. Triantis, D. Tsitsonis

MTA-ELTE Lendület CMS Particle and Nuclear Physics Group, Eötvös Loránd University, Budapest, Hungary

M. Bartók[19], M. Csanad, N. Filipovic, P. Major, M.I. Nagy, G. Pasztor, O. Surányi, G.I. Veres

Wigner Research Centre for Physics, Budapest, Hungary

G. Bencze, C. Hajdu, D. Horvath[20], Á. Hunyadi, F. Sikler, T.Á. Vámi, V. Veszpremi, G. Vesztergombi[†]

Institute of Nuclear Research ATOMKI, Debrecen, Hungary

N. Beni, S. Czellar, J. Karancsi[19], A. Makovec, J. Molnar, Z. Szillasi

Institute of Physics, University of Debrecen, Debrecen, Hungary

P. Raics, Z.L. Trocsanyi, B. Ujvari

Indian Institute of Science (IISc), Bangalore, India

S. Choudhury, J.R. Komaragiri, P.C. Tiwari

National Institute of Science Education and Research, HBNI, Bhubaneswar, India

S. Bahinipati[22], C. Kar, P. Mal, K. Mandal, A. Nayak[23], S. Roy Chowdhury, D.K. Sahoo[22], S.K. Swain

Panjab University, Chandigarh, India

S. Bansal, S.B. Beri, V. Bhatnagar, S. Chauhan, R. Chawla, N. Dhingra, R. Gupta, A. Kaur, M. Kaur, S. Kaur, P. Kumari, M. Lohan, M. Meena, A. Mehta, K. Sandeep, S. Sharma, J.B. Singh, A.K. Virdi, G. Walia

University of Delhi, Delhi, India

A. Bhardwaj, B.C. Choudhary, R.B. Garg, M. Gola, S. Keshri, Ashok Kumar, S. Malhotra, M. Naimuddin, P. Priyanka, K. Ranjan, Aashaq Shah, R. Sharma

Saha Institute of Nuclear Physics, HBNI, Kolkata, India

R. Bhardwaj[24], M. Bharti[24], R. Bhattacharya, S. Bhattacharya, U. Bhawandeep[24], D. Bhowmik, S. Dey, S. Dutt[24], S. Dutta, S. Ghosh, M. Maity[25], K. Mondal, S. Nandan, A. Purohit, P.K. Rout, A. Roy, G. Saha, S. Sarkar, T. Sarkar[25], M. Sharan, B. Singh[24], S. Thakur[24]

Indian Institute of Technology Madras, Madras, India

P.K. Behera, A. Muhammad

Bhabha Atomic Research Centre, Mumbai, India

R. Chudasama, D. Dutta, V. Jha, V. Kumar, D.K. Mishra, P.K. Netrakanti, L.M. Pant, P. Shukla, P. Suggisetti

Tata Institute of Fundamental Research-A, Mumbai, India

T. Aziz, M.A. Bhat, S. Dugad, G.B. Mohanty, N. Sur, RavindraKumar Verma

Tata Institute of Fundamental Research-B, Mumbai, India

S. Banerjee, S. Bhattacharya, S. Chatterjee, P. Das, M. Guchait, Sa. Jain, S. Karmakar, S. Kumar, G. Majumder, K. Mazumdar, N. Sahoo

Indian Institute of Science Education and Research (IISER), Pune, India

S. Chauhan, S. Dube, V. Hegde, A. Kapoor, K. Kothekar, S. Pandey, A. Rane, A. Rastogi, S. Sharma

Institute for Research in Fundamental Sciences (IPM), Tehran, Iran

S. Chenarani[26], E. Eskandari Tadavani, S.M. Etesami[26], M. Khakzad, M. Mohammadi Najafabadi, M. Naseri, F. Rezaei Hosseinabadi, B. Safarzadeh[27], M. Zeinali

University College Dublin, Dublin, Ireland

M. Felcini, M. Grunewald

INFN Sezione di Bari[a], Università di Bari[b], Politecnico di Bari[c], Bari, Italy

M. Abbrescia[a,b], C. Calabria[a,b], A. Colaleo[a], D. Creanza[a,c], L. Cristella[a,b], N. De Filippis[a,c], M. De Palma[a,b], A. Di Florio[a,b], F. Errico[a,b], L. Fiore[a], A. Gelmi[a,b], G. Iaselli[a,c], M. Ince[a,b], S. Lezki[a,b], G. Maggi[a,c], M. Maggi[a], G. Miniello[a,b], S. My[a,b], S. Nuzzo[a,b], A. Pompili[a,b], G. Pugliese[a,c], R. Radogna[a], A. Ranieri[a], G. Selvaggi[a,b], A. Sharma[a], L. Silvestris[a], R. Venditti[a], P. Verwilligen[a]

INFN Sezione di Bologna[a], Università di Bologna[b], Bologna, Italy

G. Abbiendi[a], C. Battilana[a,b], D. Bonacorsi[a,b], L. Borgonovi[a,b], S. Braibant-Giacomelli[a,b], R. Campanini[a,b], P. Capiluppi[a,b], A. Castro[a,b], F.R. Cavallo[a], S.S. Chhibra[a,b], G. Codispoti[a,b], M. Cuffiani[a,b], G.M. Dallavalle[a], F. Fabbri[a], A. Fanfani[a,b], E. Fontanesi, P. Giacomelli[a], C. Grandi[a], L. Guiducci[a,b], F. Iemmi[a,b], S. Lo Meo[a,28], S. Marcellini[a], G. Masetti[a], A. Montanari[a], F.L. Navarria[a,b], A. Perrotta[a], F. Primavera[a,b], A.M. Rossi[a,b], T. Rovelli[a,b], G.P. Siroli[a,b], N. Tosi[a]

INFN Sezione di Catania[a], Università di Catania[b], Catania, Italy

S. Albergo[a,b], A. Di Mattia[a], R. Potenza[a,b], A. Tricomi[a,b], C. Tuve[a,b]

INFN Sezione di Firenze[a], Università di Firenze[b], Firenze, Italy

G. Barbagli[a], K. Chatterjee[a,b], V. Ciulli[a,b], C. Civinini[a], R. D'Alessandro[a,b], E. Focardi[a,b], G. Latino, P. Lenzi[a,b], M. Meschini[a], S. Paoletti[a], L. Russo[a,29], G. Sguazzoni[a], D. Strom[a], L. Viliani[a]

INFN Laboratori Nazionali di Frascati, Frascati, Italy

L. Benussi, S. Bianco, F. Fabbri, D. Piccolo

INFN Sezione di Genova[a], Università di Genova[b], Genova, Italy

F. Ferro[a], R. Mulargia[a,b], E. Robutti[a], S. Tosi[a,b]

INFN Sezione di Milano-Bicocca[a], Università di Milano-Bicocca[b], Milano, Italy

A. Benaglia[a], A. Beschi[b], F. Brivio[a,b], V. Ciriolo[a,b,15], S. Di Guida[a,b,15], M.E. Dinardo[a,b], S. Fiorendi[a,b], S. Gennai[a], A. Ghezzi[a,b], P. Govoni[a,b], M. Malberti[a,b], S. Malvezzi[a], D. Menasce[a], F. Monti, L. Moroni[a], M. Paganoni[a,b], D. Pedrini[a], S. Ragazzi[a,b], T. Tabarelli de Fatis[a,b], D. Zuolo[a,b]

INFN Sezione di Napoli[a], Università di Napoli 'Federico II'[b], Napoli, Italy, Università della Basilicata[c], Potenza, Italy, Università G. Marconi[d], Roma, Italy

S. Buontempo[a], N. Cavallo[a,c], A. De Iorio[a,b], A. Di Crescenzo[a,b], F. Fabozzi[a,c], F. Fienga[a], G. Galati[a], A.O.M. Iorio[a,b], L. Lista[a], S. Meola[a,d,15], P. Paolucci[a,15], C. Sciacca[a,b], E. Voevodina[a,b]

INFN Sezione di Padova[a], Università di Padova[b], Padova, Italy, Università di Trento[c], Trento, Italy

P. Azzi[a], N. Bacchetta[a], D. Bisello[a,b], A. Boletti[a,b], A. Bragagnolo, R. Carlin[a,b], P. Checchia[a], M. Dall'Osso[a,b], P. De Castro Manzano[a], T. Dorigo[a], U. Dosselli[a], F. Gasparini[a,b], U. Gasparini[a,b], A. Gozzelino[a], S.Y. Hoh, S. Lacaprara[a], P. Lujan, M. Margoni[a,b], A.T. Meneguzzo[a,b], J. Pazzini[a,b], M. Presilla[b], P. Ronchese[a,b], R. Rossin[a,b], F. Simonetto[a,b], A. Tiko, E. Torassa[a], M. Tosi[a,b], M. Zanetti[a,b], P. Zotto[a,b], G. Zumerle[a,b]

INFN Sezione di Pavia[a], Università di Pavia[b], Pavia, Italy

A. Braghieri[a], A. Magnani[a], P. Montagna[a,b], S.P. Ratti[a,b], V. Re[a], M. Ressegotti[a,b], C. Riccardi[a,b], P. Salvini[a], I. Vai[a,b], P. Vitulo[a,b]

INFN Sezione di Perugia[a], Università di Perugia[b], Perugia, Italy

M. Biasini[a,b], G.M. Bilei[a], C. Cecchi[a,b], D. Ciangottini[a,b], L. Fanò[a,b], P. Lariccia[a,b], R. Leonardi[a,b], E. Manoni[a], G. Mantovani[a,b], V. Mariani[a,b], M. Menichelli[a], A. Rossi[a,b], A. Santocchia[a,b], D. Spiga[a]

INFN Sezione di Pisa[a], Università di Pisa[b], Scuola Normale Superiore di Pisa[c], Pisa, Italy

K. Androsov[a], P. Azzurri[a], G. Bagliesi[a], L. Bianchini[a], T. Boccali[a], L. Borrello, R. Castaldi[a], M.A. Ciocci[a,b], R. Dell'Orso[a], G. Fedi[a], F. Fiori[a,c], L. Giannini[a,c], A. Giassi[a], M.T. Grippo[a], F. Ligabue[a,c], E. Manca[a,c], G. Mandorli[a,c], A. Messineo[a,b], F. Palla[a], A. Rizzi[a,b], G. Rolandi[30], P. Spagnolo[a], R. Tenchini[a], G. Tonelli[a,b], A. Venturi[a], P.G. Verdini[a]

INFN Sezione di Roma^a, Sapienza Università di Roma^b, Rome, Italy

L. Barone^{a,b}, F. Cavallari^a, M. Cipriani^{a,b}, D. Del Re^{a,b}, E. Di Marco^{a,b}, M. Diemoz^a, S. Gelli^{a,b}, E. Longo^{a,b}, B. Marzocchi^{a,b}, P. Meridiani^a, G. Organtini^{a,b}, F. Pandolfi^a, R. Paramatti^{a,b}, F. Preiato^{a,b}, S. Rahatlou^{a,b}, C. Rovelli^a, F. Santanastasio^{a,b}

INFN Sezione di Torino^a, Università di Torino^b, Torino, Italy, Università del Piemonte Orientale^c, Novara, Italy

N. Amapane^{a,b}, R. Arcidiacono^{a,c}, S. Argiro^{a,b}, M. Arneodo^{a,c}, N. Bartosik^a, R. Bellan^{a,b}, C. Biino^a, A. Cappati^{a,b}, N. Cartiglia^a, F. Cenna^{a,b}, S. Cometti^a, M. Costa^{a,b}, R. Covarelli^{a,b}, N. Demaria^a, B. Kiani^{a,b}, C. Mariotti^a, S. Maselli^a, E. Migliore^{a,b}, V. Monaco^{a,b}, E. Monteil^{a,b}, M. Monteno^a, M.M. Obertino^{a,b}, L. Pacher^{a,b}, N. Pastrone^a, M. Pelliccioni^a, G.L. Pinna Angioni^{a,b}, A. Romero^{a,b}, M. Ruspa^{a,c}, R. Sacchi^{a,b}, R. Salvatico^{a,b}, K. Shchelina^{a,b}, V. Sola^a, A. Solano^{a,b}, D. Soldi^{a,b}, A. Staiano^a

INFN Sezione di Trieste^a, Università di Trieste^b, Trieste, Italy

S. Belforte^a, V. Candelise^{a,b}, M. Casarsa^a, F. Cossutti^a, A. Da Rold^{a,b}, G. Della Ricca^{a,b}, F. Vazzoler^{a,b}, A. Zanetti^a

Kyungpook National University, Daegu, Korea

C. Huh, D.H. Kim, G.N. Kim, M.S. Kim, J. Lee, S. Lee, S.W. Lee, C.S. Moon, Y.D. Oh, S.I. Pak, S. Sekmen, D.C. Son, Y.C. Yang

Chonnam National University, Institute for Universe and Elementary Particles, Kwangju, Korea

H. Kim, D.H. Moon, G. Oh

Hanyang University, Seoul, Korea

B. Francois, J. Goh[31], T.J. Kim

Korea University, Seoul, Korea

S. Cho, S. Choi, Y. Go, D. Gyun, S. Ha, B. Hong, Y. Jo, K. Lee, K.S. Lee, S. Lee, J. Lim, S.K. Park, Y. Roh

Sejong University, Seoul, Korea

H.S. Kim

Seoul National University, Seoul, Korea

J. Almond, J. Kim, J.S. Kim, H. Lee, K. Lee, K. Nam, S.B. Oh, B.C. Radburn-Smith, S.h. Seo, U.K. Yang, H.D. Yoo, G.B. Yu

University of Seoul, Seoul, Korea

D. Jeon, H. Kim, J.H. Kim, J.S.H. Lee, I.C. Park

Sungkyunkwan University, Suwon, Korea

Y. Choi, C. Hwang, J. Lee, I. Yu

Riga Technical University, Riga, Latvia

V. Veckalns[32]

Vilnius University, Vilnius, Lithuania

V. Dudenas, A. Juodagalvis, J. Vaitkus

National Centre for Particle Physics, Universiti Malaya, Kuala Lumpur, Malaysia

Z.A. Ibrahim, M.A.B. Md Ali[33], F. Mohamad Idris[34], W.A.T. Wan Abdullah, M.N. Yusli, Z. Zolkapli

Universidad de Sonora (UNISON), Hermosillo, Mexico

J.F. Benitez, A. Castaneda Hernandez, J.A. Murillo Quijada

Centro de Investigacion y de Estudios Avanzados del IPN, Mexico City, Mexico

H. Castilla-Valdez, E. De La Cruz-Burelo, M.C. Duran-Osuna, I. Heredia-De La Cruz[35], R. Lopez-Fernandez, J. Mejia Guisao, R.I. Rabadan-Trejo, M. Ramirez-Garcia, G. Ramirez-Sanchez, R. Reyes-Almanza, A. Sanchez-Hernandez

Universidad Iberoamericana, Mexico City, Mexico

S. Carrillo Moreno, C. Oropeza Barrera, F. Vazquez Valencia

Benemerita Universidad Autonoma de Puebla, Puebla, Mexico

J. Eysermans, I. Pedraza, H.A. Salazar Ibarguen, C. Uribe Estrada

Universidad Autónoma de San Luis Potosí, San Luis Potosí, Mexico

A. Morelos Pineda

University of Auckland, Auckland, New Zealand

D. Krofcheck

University of Canterbury, Christchurch, New Zealand

S. Bheesette, P.H. Butler

National Centre for Physics, Quaid-I-Azam University, Islamabad, Pakistan

A. Ahmad, M. Ahmad, M.I. Asghar, Q. Hassan, H.R. Hoorani, W.A. Khan, M.A. Shah, M. Shoaib, M. Waqas

National Centre for Nuclear Research, Swierk, Poland

H. Bialkowska, M. Bluj, B. Boimska, T. Frueboes, M. Górski, M. Kazana, M. Szleper, P. Traczyk, P. Zalewski

Institute of Experimental Physics, Faculty of Physics, University of Warsaw, Warsaw, Poland

K. Bunkowski, A. Byszuk[36], K. Doroba, A. Kalinowski, M. Konecki, J. Krolikowski, M. Misiura, M. Olszewski, A. Pyskir, M. Walczak

Laboratório de Instrumentação e Física Experimental de Partículas, Lisboa, Portugal

M. Araujo, P. Bargassa, C. Beirão Da Cruz E Silva, A. Di Francesco, P. Faccioli, B. Galinhas, M. Gallinaro, J. Hollar, N. Leonardo, J. Seixas, G. Strong, O. Toldaiev, J. Varela

Joint Institute for Nuclear Research, Dubna, Russia

S. Afanasiev, P. Bunin, M. Gavrilenko, I. Golutvin, I. Gorbunov, A. Kamenev, V. Karjavine, A. Lanev, A. Malakhov, V. Matveev[37,38], P. Moisenz, V. Palichik, V. Perelygin, S. Shmatov, S. Shulha, N. Skatchkov, V. Smirnov, N. Voytishin, A. Zarubin

Petersburg Nuclear Physics Institute, Gatchina (St. Petersburg), Russia

V. Golovtsov, Y. Ivanov, V. Kim[39], E. Kuznetsova[40], P. Levchenko, V. Murzin, V. Oreshkin, I. Smirnov, D. Sosnov, V. Sulimov, L. Uvarov, S. Vavilov, A. Vorobyev

Institute for Nuclear Research, Moscow, Russia

Yu. Andreev, A. Dermenev, S. Gninenko, N. Golubev, A. Karneyeu, M. Kirsanov, N. Krasnikov, A. Pashenkov, A. Shabanov, D. Tlisov, A. Toropin

Institute for Theoretical and Experimental Physics, Moscow, Russia

V. Epshteyn, V. Gavrilov, N. Lychkovskaya, V. Popov, I. Pozdnyakov, G. Safronov, A. Spiridonov, A. Stepennov, V. Stolin, M. Toms, E. Vlasov, A. Zhokin

Moscow Institute of Physics and Technology, Moscow, Russia

T. Aushev

National Research Nuclear University 'Moscow Engineering Physics Institute' (MEPhI), Moscow, Russia

M. Chadeeva[41], S. Polikarpov[41], E. Popova, V. Rusinov

P.N. Lebedev Physical Institute, Moscow, Russia

V. Andreev, M. Azarkin, I. Dremin[38], M. Kirakosyan, A. Terkulov

Skobeltsyn Institute of Nuclear Physics, Lomonosov Moscow State University, Moscow, Russia

A. Belyaev, E. Boos, M. Dubinin[42], L. Dudko, A. Ershov, A. Gribushin, V. Klyukhin, O. Kodolova, I. Lokhtin, S. Obraztsov, S. Petrushanko, V. Savrin, A. Snigirev

Novosibirsk State University (NSU), Novosibirsk, Russia

A. Barnyakov[43], V. Blinov[43], T. Dimova[43], L. Kardapoltsev[43], Y. Skovpen[43]

Institute for High Energy Physics of National Research Centre 'Kurchatov Institute', Protvino, Russia

I. Azhgirey, I. Bayshev, S. Bitioukov, V. Kachanov, A. Kalinin, D. Konstantinov, P. Mandrik, V. Petrov, R. Ryutin, S. Slabospitskii, A. Sobol, S. Troshin, N. Tyurin, A. Uzunian, A. Volkov

National Research Tomsk Polytechnic University, Tomsk, Russia

A. Babaev, S. Baidali, V. Okhotnikov

University of Belgrade, Faculty of Physics and Vinca Institute of Nuclear Sciences, Belgrade, Serbia

P. Adzic[44], P. Cirkovic, D. Devetak, M. Dordevic, P. Milenovic[45], J. Milosevic

Centro de Investigaciones Energéticas Medioambientales y Tecnológicas (CIEMAT), Madrid, Spain

J. Alcaraz Maestre, A. Álvarez Fernández, I. Bachiller, M. Barrio Luna, J.A. Brochero Cifuentes, M. Cerrada, N. Colino, B. De La Cruz, A. Delgado Peris, C. Fernandez Bedoya, J.P. Fernández Ramos, J. Flix, M.C. Fouz, O. Gonzalez Lopez, S. Goy Lopez, J.M. Hernandez, M.I. Josa, D. Moran, A. Pérez-Calero Yzquierdo, J. Puerta Pelayo, I. Redondo, L. Romero, S. Sánchez Navas, M.S. Soares, A. Triossi

Universidad Autónoma de Madrid, Madrid, Spain

C. Albajar, J.F. de Trocóniz

Universidad de Oviedo, Oviedo, Spain

J. Cuevas, C. Erice, J. Fernandez Menendez, S. Folgueras, I. Gonzalez Caballero, J.R. González Fernández, E. Palencia Cortezon, V. Rodríguez Bouza, S. Sanchez Cruz, J.M. Vizan Garcia

Instituto de Física de Cantabria (IFCA), CSIC-Universidad de Cantabria, Santander, Spain

I.J. Cabrillo, A. Calderon, B. Chazin Quero, J. Duarte Campderros, M. Fernandez, P.J. Fernández Manteca, A. García Alonso, J. Garcia-Ferrero, G. Gomez, A. Lopez Virto, J. Marco, C. Martinez Rivero, P. Martinez Ruiz del Arbol, F. Matorras, J. Piedra Gomez, C. Prieels, T. Rodrigo, A. Ruiz-Jimeno, L. Scodellaro, N. Trevisani, I. Vila, R. Vilar Cortabitarte

University of Ruhuna, Department of Physics, Matara, Sri Lanka

N. Wickramage

CERN, European Organization for Nuclear Research, Geneva, Switzerland

D. Abbaneo, B. Akgun, E. Auffray, G. Auzinger, P. Baillon, A.H. Ball, D. Barney, J. Bendavid, M. Bianco, A. Bocci, C. Botta, E. Brondolin, T. Camporesi, M. Cepeda, G. Cerminara, E. Chapon, Y. Chen, G. Cucciati, D. d'Enterria, A. Dabrowski, N. Daci, V. Daponte, A. David, A. De Roeck, N. Deelen, M. Dobson, M. Dünser, N. Dupont, A. Elliott-Peisert, F. Fallavollita[46], D. Fasanella, G. Franzoni, J. Fulcher, W. Funk, D. Gigi, A. Gilbert, K. Gill, F. Glege, M. Gruchala, M. Guilbaud, D. Gulhan, J. Hegeman, C. Heidegger, V. Innocente, G.M. Innocenti, A. Jafari, P. Janot, O. Karacheban[18], J. Kieseler, A. Kornmayer, M. Krammer[1], C. Lange, P. Lecoq, C. Lourenço, L. Malgeri, M. Mannelli, A. Massironi, F. Meijers, J.A. Merlin, S. Mersi, E. Meschi, F. Moortgat, M. Mulders, J. Ngadiuba, S. Nourbakhsh, S. Orfanelli, L. Orsini, F. Pantaleo[15], L. Pape, E. Perez, M. Peruzzi, A. Petrilli, G. Petrucciani, A. Pfeiffer, M. Pierini, F.M. Pitters, D. Rabady, A. Racz, T. Reis, M. Rovere, H. Sakulin, C. Schäfer, C. Schwick, M. Selvaggi, A. Sharma, P. Silva, P. Sphicas[47], A. Stakia, J. Steggemann, D. Treille, A. Tsirou, A. Vartak, M. Verzetti, W.D. Zeuner

Paul Scherrer Institut, Villigen, Switzerland

L. Caminada[48], K. Deiters, W. Erdmann, R. Horisberger, Q. Ingram, H.C. Kaestli, D. Kotlinski, U. Langenegger, T. Rohe, S.A. Wiederkehr

ETH Zurich — Institute for Particle Physics and Astrophysics (IPA), Zurich, Switzerland

M. Backhaus, L. Bäni, P. Berger, N. Chernyavskaya, G. Dissertori, M. Dittmar, M. Donegà, C. Dorfer, T.A. Gómez Espinosa, C. Grab, D. Hits, T. Klijnsma, W. Lustermann, R.A. Manzoni, M. Marionneau, M.T. Meinhard, F. Micheli, P. Musella, F. Nessi-Tedaldi, F. Pauss, G. Perrin, L. Perrozzi, S. Pigazzini, M. Reichmann, C. Reissel, D. Ruini, D.A. Sanz Becerra, M. Schönenberger, L. Shchutska, V.R. Tavolaro, K. Theofilatos, M.L. Vesterbacka Olsson, R. Wallny, D.H. Zhu

Universität Zürich, Zurich, Switzerland

T.K. Aarrestad, C. Amsler[49], D. Brzhechko, M.F. Canelli, A. De Cosa, R. Del Burgo, S. Donato, C. Galloni, T. Hreus, B. Kilminster, S. Leontsinis, I. Neutelings, G. Rauco, P. Robmann, D. Salerno, K. Schweiger, C. Seitz, Y. Takahashi, S. Wertz, A. Zucchetta

National Central University, Chung-Li, Taiwan

T.H. Doan, R. Khurana, C.M. Kuo, W. Lin, A. Pozdnyakov, S.S. Yu

National Taiwan University (NTU), Taipei, Taiwan

P. Chang, Y. Chao, K.F. Chen, P.H. Chen, W.-S. Hou, Y.F. Liu, R.-S. Lu, E. Paganis, A. Psallidas, A. Steen

Chulalongkorn University, Faculty of Science, Department of Physics, Bangkok, Thailand

B. Asavapibhop, N. Srimanobhas, N. Suwonjandee

Çukurova University, Physics Department, Science and Art Faculty, Adana, Turkey

A. Bat, F. Boran, S. Cerci[50], S. Damarseckin, Z.S. Demiroglu, F. Dolek, C. Dozen, I. Dumanoglu, G. Gokbulut, Y. Guler, E. Gurpinar, I. Hos[51], C. Isik, E.E. Kangal[52], O. Kara, A. Kayis Topaksu, U. Kiminsu, M. Oglakci, G. Onengut, K. Ozdemir[53], S. Ozturk[54], D. Sunar Cerci[50], B. Tali[50], U.G. Tok, S. Turkcapar, I.S. Zorbakir, C. Zorbilmez

Middle East Technical University, Physics Department, Ankara, Turkey

B. Isildak[55], G. Karapinar[56], M. Yalvac, M. Zeyrek

Bogazici University, Istanbul, Turkey

I.O. Atakisi, E. Gülmez, M. Kaya[57], O. Kaya[58], S. Ozkorucuklu[59], S. Tekten, E.A. Yetkin[60]

Istanbul Technical University, Istanbul, Turkey

M.N. Agaras, A. Cakir, K. Cankocak, Y. Komurcu, S. Sen[61]

Institute for Scintillation Materials of National Academy of Science of Ukraine, Kharkov, Ukraine

B. Grynyov

National Scientific Center, Kharkov Institute of Physics and Technology, Kharkov, Ukraine

L. Levchuk

University of Bristol, Bristol, United Kingdom

F. Ball, J.J. Brooke, D. Burns, E. Clement, D. Cussans, O. Davignon, H. Flacher, J. Goldstein, G.P. Heath, H.F. Heath, L. Kreczko, D.M. Newbold[62], S. Paramesvaran, B. Penning, T. Sakuma, D. Smith, V.J. Smith, J. Taylor, A. Titterton

Rutherford Appleton Laboratory, Didcot, United Kingdom

K.W. Bell, A. Belyaev[63], C. Brew, R.M. Brown, D. Cieri, D.J.A. Cockerill, J.A. Coughlan, K. Harder, S. Harper, J. Linacre, K. Manolopoulos, E. Olaiya, D. Petyt, T. Schuh, C.H. Shepherd-Themistocleous, A. Thea, I.R. Tomalin, T. Williams, W.J. Womersley

Imperial College, London, United Kingdom

R. Bainbridge, P. Bloch, J. Borg, S. Breeze, O. Buchmuller, A. Bundock, D. Colling, P. Dauncey, G. Davies, M. Della Negra, R. Di Maria, P. Everaerts, G. Hall, G. Iles, T. James, M. Komm, C. Laner, L. Lyons, A.-M. Magnan, S. Malik, A. Martelli, J. Nash[64], A. Nikitenko[7], V. Palladino, M. Pesaresi, D.M. Raymond, A. Richards, A. Rose, E. Scott, C. Seez, A. Shtipliyski, G. Singh, M. Stoye, T. Strebler, S. Summers, A. Tapper, K. Uchida, T. Virdee[15], N. Wardle, D. Winterbottom, J. Wright, S.C. Zenz

Brunel University, Uxbridge, United Kingdom

J.E. Cole, P.R. Hobson, A. Khan, P. Kyberd, C.K. Mackay, A. Morton, I.D. Reid, L. Teodorescu, S. Zahid

Baylor University, Waco, U.S.A.

K. Call, J. Dittmann, K. Hatakeyama, H. Liu, C. Madrid, B. McMaster, N. Pastika, C. Smith

Catholic University of America, Washington, DC, U.S.A.

R. Bartek, A. Dominguez

The University of Alabama, Tuscaloosa, U.S.A.

A. Buccilli, S.I. Cooper, C. Henderson, P. Rumerio, C. West

Boston University, Boston, U.S.A.

D. Arcaro, T. Bose, D. Gastler, S. Girgis, D. Pinna, C. Richardson, J. Rohlf, L. Sulak, D. Zou

Brown University, Providence, U.S.A.

G. Benelli, B. Burkle, X. Coubez, D. Cutts, M. Hadley, J. Hakala, U. Heintz, J.M. Hogan[65], K.H.M. Kwok, E. Laird, G. Landsberg, J. Lee, Z. Mao, M. Narain, S. Sagir[66], R. Syarif, E. Usai, D. Yu

University of California, Davis, Davis, U.S.A.

R. Band, C. Brainerd, R. Breedon, D. Burns, M. Calderon De La Barca Sanchez, M. Chertok, J. Conway, R. Conway, P.T. Cox, R. Erbacher, C. Flores, G. Funk, W. Ko, O. Kukral, R. Lander, M. Mulhearn, D. Pellett, J. Pilot, S. Shalhout, M. Shi, D. Stolp, D. Taylor, K. Tos, M. Tripathi, Z. Wang, F. Zhang

University of California, Los Angeles, U.S.A.

M. Bachtis, C. Bravo, R. Cousins, A. Dasgupta, S. Erhan, A. Florent, J. Hauser, M. Ignatenko, N. Mccoll, S. Regnard, D. Saltzberg, C. Schnaible, V. Valuev

University of California, Riverside, Riverside, U.S.A.

E. Bouvier, K. Burt, R. Clare, J.W. Gary, S.M.A. Ghiasi Shirazi, G. Hanson, G. Karapostoli, E. Kennedy, F. Lacroix, O.R. Long, M. Olmedo Negrete, M.I. Paneva, W. Si, L. Wang, H. Wei, S. Wimpenny, B.R. Yates

University of California, San Diego, La Jolla, U.S.A.

J.G. Branson, P. Chang, S. Cittolin, M. Derdzinski, R. Gerosa, D. Gilbert, B. Hashemi, A. Holzner, D. Klein, G. Kole, V. Krutelyov, J. Letts, M. Masciovecchio, S. May, D. Olivito, S. Padhi, M. Pieri, V. Sharma, M. Tadel, J. Wood, F. Würthwein, A. Yagil, G. Zevi Della Porta

University of California, Santa Barbara — Department of Physics, Santa Barbara, U.S.A.

N. Amin, R. Bhandari, C. Campagnari, M. Citron, V. Dutta, M. Franco Sevilla, L. Gouskos, R. Heller, J. Incandela, H. Mei, A. Ovcharova, H. Qu, J. Richman, D. Stuart, I. Suarez, S. Wang, J. Yoo

California Institute of Technology, Pasadena, U.S.A.

D. Anderson, A. Bornheim, J.M. Lawhorn, N. Lu, H.B. Newman, T.Q. Nguyen, J. Pata, M. Spiropulu, J.R. Vlimant, R. Wilkinson, S. Xie, Z. Zhang, R.Y. Zhu

Carnegie Mellon University, Pittsburgh, U.S.A.

M.B. Andrews, T. Ferguson, T. Mudholkar, M. Paulini, M. Sun, I. Vorobiev, M. Weinberg

University of Colorado Boulder, Boulder, U.S.A.

J.P. Cumalat, W.T. Ford, F. Jensen, A. Johnson, E. MacDonald, T. Mulholland, R. Patel, A. Perloff, K. Stenson, K.A. Ulmer, S.R. Wagner

Cornell University, Ithaca, U.S.A.

J. Alexander, J. Chaves, Y. Cheng, J. Chu, A. Datta, K. Mcdermott, N. Mirman, J.R. Patterson, D. Quach, A. Rinkevicius, A. Ryd, L. Skinnari, L. Soffi, S.M. Tan, Z. Tao, J. Thom, J. Tucker, P. Wittich, M. Zientek

Fermi National Accelerator Laboratory, Batavia, U.S.A.

S. Abdullin, M. Albrow, M. Alyari, G. Apollinari, A. Apresyan, A. Apyan, S. Banerjee, L.A.T. Bauerdick, A. Beretvas, J. Berryhill, P.C. Bhat, K. Burkett, J.N. Butler, A. Canepa, G.B. Cerati, H.W.K. Cheung, F. Chlebana, M. Cremonesi, J. Duarte, V.D. Elvira, J. Freeman, Z. Gecse, E. Gottschalk, L. Gray, D. Green, S. Grünendahl, O. Gutsche, J. Hanlon, R.M. Harris, S. Hasegawa, J. Hirschauer, Z. Hu, B. Jayatilaka, S. Jindariani, M. Johnson, U. Joshi, B. Klima, M.J. Kortelainen, B. Kreis, S. Lammel, D. Lincoln, R. Lipton, M. Liu, T. Liu, J. Lykken, K. Maeshima, J.M. Marraffino, D. Mason, P. McBride, P. Merkel, S. Mrenna, S. Nahn, V. O'Dell, K. Pedro, C. Pena, O. Prokofyev, G. Rakness, F. Ravera, A. Reinsvold, L. Ristori, A. Savoy-Navarro[67], B. Schneider, E. Sexton-Kennedy,

A. Soha, W.J. Spalding, L. Spiegel, S. Stoynev, J. Strait, N. Strobbe, L. Taylor, S. Tkaczyk, N.V. Tran, L. Uplegger, E.W. Vaandering, C. Vernieri, M. Verzocchi, R. Vidal, M. Wang, H.A. Weber

University of Florida, Gainesville, U.S.A.

D. Acosta, P. Avery, P. Bortignon, D. Bourilkov, A. Brinkerhoff, L. Cadamuro, A. Carnes, D. Curry, R.D. Field, S.V. Gleyzer, B.M. Joshi, J. Konigsberg, A. Korytov, K.H. Lo, P. Ma, K. Matchev, N. Menendez, G. Mitselmakher, D. Rosenzweig, K. Shi, D. Sperka, J. Wang, S. Wang, X. Zuo

Florida International University, Miami, U.S.A.

Y.R. Joshi, S. Linn

Florida State University, Tallahassee, U.S.A.

A. Ackert, T. Adams, A. Askew, S. Hagopian, V. Hagopian, K.F. Johnson, T. Kolberg, G. Martinez, T. Perry, H. Prosper, A. Saha, C. Schiber, R. Yohay

Florida Institute of Technology, Melbourne, U.S.A.

M.M. Baarmand, V. Bhopatkar, S. Colafranceschi, M. Hohlmann, D. Noonan, M. Rahmani, T. Roy, M. Saunders, F. Yumiceva

University of Illinois at Chicago (UIC), Chicago, U.S.A.

M.R. Adams, L. Apanasevich, D. Berry, R.R. Betts, R. Cavanaugh, X. Chen, S. Dittmer, O. Evdokimov, C.E. Gerber, D.A. Hangal, D.J. Hofman, K. Jung, J. Kamin, C. Mills, M.B. Tonjes, N. Varelas, H. Wang, X. Wang, Z. Wu, J. Zhang

The University of Iowa, Iowa City, U.S.A.

M. Alhusseini, B. Bilki[68], W. Clarida, K. Dilsiz[69], S. Durgut, R.P. Gandrajula, M. Haytmyradov, V. Khristenko, J.-P. Merlo, A. Mestvirishvili, A. Moeller, J. Nachtman, H. Ogul[70], Y. Onel, F. Ozok[71], A. Penzo, C. Snyder, E. Tiras, J. Wetzel

Johns Hopkins University, Baltimore, U.S.A.

B. Blumenfeld, A. Cocoros, N. Eminizer, D. Fehling, L. Feng, A.V. Gritsan, W.T. Hung, P. Maksimovic, J. Roskes, U. Sarica, M. Swartz, M. Xiao

The University of Kansas, Lawrence, U.S.A.

A. Al-bataineh, P. Baringer, A. Bean, S. Boren, J. Bowen, A. Bylinkin, J. Castle, S. Khalil, A. Kropivnitskaya, D. Majumder, W. Mcbrayer, M. Murray, C. Rogan, S. Sanders, E. Schmitz, J.D. Tapia Takaki, Q. Wang

Kansas State University, Manhattan, U.S.A.

S. Duric, A. Ivanov, K. Kaadze, D. Kim, Y. Maravin, D.R. Mendis, T. Mitchell, A. Modak, A. Mohammadi

Lawrence Livermore National Laboratory, Livermore, U.S.A.

F. Rebassoo, D. Wright

University of Maryland, College Park, U.S.A.

A. Baden, O. Baron, A. Belloni, S.C. Eno, Y. Feng, C. Ferraioli, N.J. Hadley, S. Jabeen, G.Y. Jeng, R.G. Kellogg, J. Kunkle, A.C. Mignerey, S. Nabili, F. Ricci-Tam, M. Seidel, Y.H. Shin, A. Skuja, S.C. Tonwar, K. Wong

Massachusetts Institute of Technology, Cambridge, U.S.A.

D. Abercrombie, B. Allen, V. Azzolini, A. Baty, R. Bi, S. Brandt, W. Busza, I.A. Cali, M. D'Alfonso, Z. Demiragli, G. Gomez Ceballos, M. Goncharov, P. Harris, D. Hsu, M. Hu, Y. Iiyama, M. Klute, D. Kovalskyi, Y.-J. Lee, P.D. Luckey, B. Maier, A.C. Marini, C. Mcginn, C. Mironov, S. Narayanan, X. Niu, C. Paus, D. Rankin, C. Roland, G. Roland, Z. Shi, G.S.F. Stephans, K. Sumorok, K. Tatar, D. Velicanu, J. Wang, T.W. Wang, B. Wyslouch

University of Minnesota, Minneapolis, U.S.A.

A.C. Benvenuti[†], R.M. Chatterjee, A. Evans, P. Hansen, J. Hiltbrand, Sh. Jain, S. Kalafut, M. Krohn, Y. Kubota, Z. Lesko, J. Mans, R. Rusack, M.A. Wadud

University of Mississippi, Oxford, U.S.A.

J.G. Acosta, S. Oliveros

University of Nebraska-Lincoln, Lincoln, U.S.A.

E. Avdeeva, K. Bloom, D.R. Claes, C. Fangmeier, F. Golf, R. Gonzalez Suarez, R. Kamalieddin, I. Kravchenko, J. Monroy, J.E. Siado, G.R. Snow, B. Stieger

State University of New York at Buffalo, Buffalo, U.S.A.

A. Godshalk, C. Harrington, I. Iashvili, A. Kharchilava, C. Mclean, D. Nguyen, A. Parker, S. Rappoccio, B. Roozbahani

Northeastern University, Boston, U.S.A.

G. Alverson, E. Barberis, C. Freer, Y. Haddad, A. Hortiangtham, G. Madigan, D.M. Morse, T. Orimoto, A. Tishelman-charny, T. Wamorkar, B. Wang, A. Wisecarver, D. Wood

Northwestern University, Evanston, U.S.A.

S. Bhattacharya, J. Bueghly, O. Charaf, T. Gunter, K.A. Hahn, N. Odell, M.H. Schmitt, K. Sung, M. Trovato, M. Velasco

University of Notre Dame, Notre Dame, U.S.A.

R. Bucci, N. Dev, R. Goldouzian, M. Hildreth, K. Hurtado Anampa, C. Jessop, D.J. Karmgard, K. Lannon, W. Li, N. Loukas, N. Marinelli, F. Meng, C. Mueller, Y. Musienko[37], M. Planer, R. Ruchti, P. Siddireddy, G. Smith, S. Taroni, M. Wayne, A. Wightman, M. Wolf, A. Woodard

The Ohio State University, Columbus, U.S.A.

J. Alimena, L. Antonelli, B. Bylsma, L.S. Durkin, S. Flowers, B. Francis, C. Hill, W. Ji, T.Y. Ling, W. Luo, B.L. Winer

Princeton University, Princeton, U.S.A.

S. Cooperstein, P. Elmer, J. Hardenbrook, N. Haubrich, S. Higginbotham, A. Kalogeropoulos, S. Kwan, D. Lange, M.T. Lucchini, J. Luo, D. Marlow, K. Mei, I. Ojalvo, J. Olsen, C. Palmer, P. Piroué, J. Salfeld-Nebgen, D. Stickland, C. Tully

University of Puerto Rico, Mayaguez, U.S.A.

S. Malik, S. Norberg

Purdue University, West Lafayette, U.S.A.

A. Barker, V.E. Barnes, S. Das, L. Gutay, M. Jones, A.W. Jung, A. Khatiwada, B. Mahakud, D.H. Miller, N. Neumeister, C.C. Peng, S. Piperov, H. Qiu, J.F. Schulte, J. Sun, F. Wang, R. Xiao, W. Xie

Purdue University Northwest, Hammond, U.S.A.

T. Cheng, J. Dolen, N. Parashar

Rice University, Houston, U.S.A.

Z. Chen, K.M. Ecklund, S. Freed, F.J.M. Geurts, M. Kilpatrick, Arun Kumar, W. Li, B.P. Padley, R. Redjimi, J. Roberts, J. Rorie, W. Shi, Z. Tu, A. Zhang

University of Rochester, Rochester, U.S.A.

A. Bodek, P. de Barbaro, R. Demina, Y.t. Duh, J.L. Dulemba, C. Fallon, T. Ferbel, M. Galanti, A. Garcia-Bellido, J. Han, O. Hindrichs, A. Khukhunaishvili, E. Ranken, P. Tan, R. Taus

Rutgers, The State University of New Jersey, Piscataway, U.S.A.

B. Chiarito, J.P. Chou, Y. Gershtein, E. Halkiadakis, A. Hart, M. Heindl, E. Hughes, S. Kaplan, R. Kunnawalkam Elayavalli, S. Kyriacou, I. Laflotte, A. Lath, R. Montalvo, K. Nash, M. Osherson, H. Saka, S. Salur, S. Schnetzer, D. Sheffield, S. Somalwar, R. Stone, S. Thomas, P. Thomassen

University of Tennessee, Knoxville, U.S.A.

H. Acharya, A.G. Delannoy, J. Heideman, G. Riley, S. Spanier

Texas A&M University, College Station, U.S.A.

O. Bouhali[72], A. Celik, M. Dalchenko, M. De Mattia, A. Delgado, S. Dildick, R. Eusebi, J. Gilmore, T. Huang, T. Kamon[73], S. Luo, D. Marley, R. Mueller, D. Overton, L. Perniè, D. Rathjens, A. Safonov

Texas Tech University, Lubbock, U.S.A.

N. Akchurin, J. Damgov, F. De Guio, P.R. Dudero, S. Kunori, K. Lamichhane, S.W. Lee, T. Mengke, S. Muthumuni, T. Peltola, S. Undleeb, I. Volobouev, Z. Wang, A. Whitbeck

Vanderbilt University, Nashville, U.S.A.

S. Greene, A. Gurrola, R. Janjam, W. Johns, C. Maguire, A. Melo, H. Ni, K. Padeken, F. Romeo, P. Sheldon, S. Tuo, J. Velkovska, M. Verweij, Q. Xu

University of Virginia, Charlottesville, U.S.A.

M.W. Arenton, P. Barria, B. Cox, R. Hirosky, M. Joyce, A. Ledovskoy, H. Li, C. Neu, T. Sinthuprasith, Y. Wang, E. Wolfe, F. Xia

Wayne State University, Detroit, U.S.A.

R. Harr, P.E. Karchin, N. Poudyal, J. Sturdy, P. Thapa, S. Zaleski

University of Wisconsin — Madison, Madison, WI, U.S.A.

J. Buchanan, C. Caillol, D. Carlsmith, S. Dasu, I. De Bruyn, L. Dodd, B. Gomber[74], M. Grothe, M. Herndon, A. Hervé, U. Hussain, P. Klabbers, A. Lanaro, K. Long, R. Loveless, T. Ruggles, A. Savin, V. Sharma, N. Smith, W.H. Smith, N. Woods

†: Deceased
1: Also at Vienna University of Technology, Vienna, Austria
2: Also at IRFU, CEA, Université Paris-Saclay, Gif-sur-Yvette, France
3: Also at Universidade Estadual de Campinas, Campinas, Brazil
4: Also at Federal University of Rio Grande do Sul, Porto Alegre, Brazil
5: Also at Université Libre de Bruxelles, Bruxelles, Belgium
6: Also at University of Chinese Academy of Sciences, Beijing, China
7: Also at Institute for Theoretical and Experimental Physics, Moscow, Russia
8: Also at Joint Institute for Nuclear Research, Dubna, Russia
9: Also at Suez University, Suez, Egypt
10: Now at British University in Egypt, Cairo, Egypt
11: Also at Zewail City of Science and Technology, Zewail, Egypt
12: Also at Department of Physics, King Abdulaziz University, Jeddah, Saudi Arabia
13: Also at Université de Haute Alsace, Mulhouse, France
14: Also at Skobeltsyn Institute of Nuclear Physics, Lomonosov Moscow State University, Moscow, Russia
15: Also at CERN, European Organization for Nuclear Research, Geneva, Switzerland
16: Also at RWTH Aachen University, III. Physikalisches Institut A, Aachen, Germany
17: Also at University of Hamburg, Hamburg, Germany
18: Also at Brandenburg University of Technology, Cottbus, Germany
19: Also at Institute of Physics, University of Debrecen, Debrecen, Hungary
20: Also at Institute of Nuclear Research ATOMKI, Debrecen, Hungary
21: Also at MTA-ELTE Lendület CMS Particle and Nuclear Physics Group, Eötvös Loránd University, Budapest, Hungary
22: Also at Indian Institute of Technology Bhubaneswar, Bhubaneswar, India
23: Also at Institute of Physics, Bhubaneswar, India
24: Also at Shoolini University, Solan, India
25: Also at University of Visva-Bharati, Santiniketan, India
26: Also at Isfahan University of Technology, Isfahan, Iran
27: Also at Plasma Physics Research Center, Science and Research Branch, Islamic Azad University, Tehran, Iran
28: Also at ITALIAN NATIONAL AGENCY FOR NEW TECHNOLOGIES, ENERGY AND SUSTAINABLE ECONOMIC DEVELOPMENT, Bologna, Italy
29: Also at Università degli Studi di Siena, Siena, Italy
30: Also at Scuola Normale e Sezione dell'INFN, Pisa, Italy
31: Also at Kyunghee University, Seoul, Korea

32: Also at Riga Technical University, Riga, Latvia

33: Also at International Islamic University of Malaysia, Kuala Lumpur, Malaysia

34: Also at Malaysian Nuclear Agency, MOSTI, Kajang, Malaysia

35: Also at Consejo Nacional de Ciencia y Tecnología, Mexico City, Mexico

36: Also at Warsaw University of Technology, Institute of Electronic Systems, Warsaw, Poland

37: Also at Institute for Nuclear Research, Moscow, Russia

38: Now at National Research Nuclear University 'Moscow Engineering Physics Institute' (MEPhI), Moscow, Russia

39: Also at St. Petersburg State Polytechnical University, St. Petersburg, Russia

40: Also at University of Florida, Gainesville, U.S.A.

41: Also at P.N. Lebedev Physical Institute, Moscow, Russia

42: Also at California Institute of Technology, Pasadena, U.S.A.

43: Also at Budker Institute of Nuclear Physics, Novosibirsk, Russia

44: Also at Faculty of Physics, University of Belgrade, Belgrade, Serbia

45: Also at University of Belgrade, Faculty of Physics and Vinca Institute of Nuclear Sciences, Belgrade, Serbia

46: Also at INFN Sezione di Pavia^a, Università di Pavia^b, Pavia, Italy

47: Also at National and Kapodistrian University of Athens, Athens, Greece

48: Also at Universität Zürich, Zurich, Switzerland

49: Also at Stefan Meyer Institute for Subatomic Physics (SMI), Vienna, Austria

50: Also at Adiyaman University, Adiyaman, Turkey

51: Also at Istanbul Aydin University, Istanbul, Turkey

52: Also at Mersin University, Mersin, Turkey

53: Also at Piri Reis University, Istanbul, Turkey

54: Also at Gaziosmanpasa University, Tokat, Turkey

55: Also at Ozyegin University, Istanbul, Turkey

56: Also at Izmir Institute of Technology, Izmir, Turkey

57: Also at Marmara University, Istanbul, Turkey

58: Also at Kafkas University, Kars, Turkey

59: Also at Istanbul University, Faculty of Science, Istanbul, Turkey

60: Also at Istanbul Bilgi University, Istanbul, Turkey

61: Also at Hacettepe University, Ankara, Turkey

62: Also at Rutherford Appleton Laboratory, Didcot, United Kingdom

63: Also at School of Physics and Astronomy, University of Southampton, Southampton, United Kingdom

64: Also at Monash University, Faculty of Science, Clayton, Australia

65: Also at Bethel University, St. Paul, U.S.A.

66: Also at Karamanoğlu Mehmetbey University, Karaman, Turkey

67: Also at Purdue University, West Lafayette, U.S.A.

68: Also at Beykent University, Istanbul, Turkey

69: Also at Bingol University, Bingol, Turkey

70: Also at Sinop University, Sinop, Turkey

71: Also at Mimar Sinan University, Istanbul, Istanbul, Turkey

72: Also at Texas A&M University at Qatar, Doha, Qatar

73: Also at Kyungpook National University, Daegu, Korea

74: Also at University of Hyderabad, Hyderabad, India